



# **Modeling and Simulation on SOL-Divertor Plasmas**

**T. Takizuka**

*Japan Atomic Energy Agency, Naka Fusion Institute*

---

ITER International Summer School 2009 (IISS2009)  
“Plasma Surface Interaction in Controlled Fusion Devices”  
22 - 26 June 2009, Aix en Provence, France

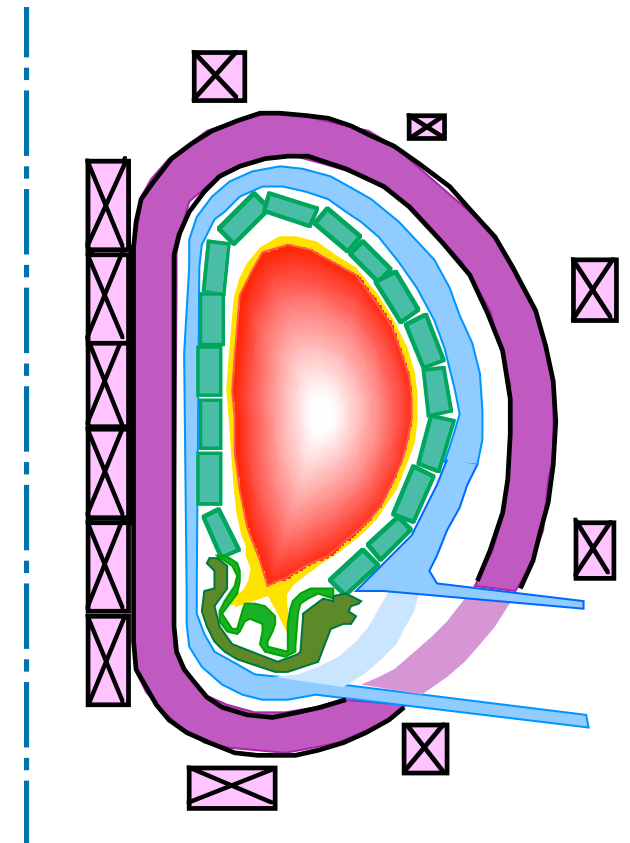
# Edge Plasma Research for Fusion

---

Hot plasma in the core region is transported across magnetic field lines to the peripheral region (closed field), and brought out to the scrape-off-layer region.

Since SOL/divertor plasmas attach walls directly, plasma particles and heat escape to the walls mainly along magnetic field lines (open field).

Utilizing this nature, we expect divertor functions for the **heat removal**, **ash exhaust**, and **impurity shielding (retention)** in fusion reactors, such as ITER and DEMO.



# Large heat flux to PFCs in fusion reactor

---

Large heat flux to the plasma facing components (PFCs) in the fusion reactor, especially to the divertor plates, is worried about the most from the viewpoint of lifetime reduction of PFCs.

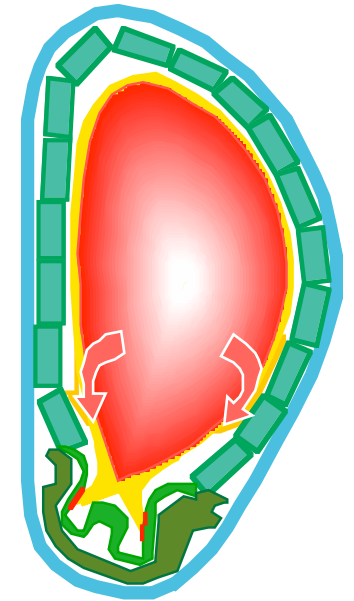
Commercial tokamak reactor with 1 GW electric power  
Fusion power  $\sim 3$  GW and Heating power 600 - 700 MW  
For radiation power  $\sim 85\%$  : Power to plates  $\sim 100$  MW  
For heat flux width  $\sim 10$  cm: Heat load to plates  $\sim 15$  MW/m<sup>2</sup>  
(  $R \sim 7$  m,  $L_{\text{plates}} \sim 60$  m,  $S_{\text{plates}} \sim 6$  m<sup>2</sup> )

Heat conductivity of SS / W : 20 / 160 W/m $\cdot$ °K /

Melting point of SS / W : 1400 / 3400 °C

Maximum heat load of SS / W : 2 / 40 MW/m<sup>2</sup>  
(with 1 cm thickness)

From the engineering viewpoint, allowable limit is smaller than these maximum values.



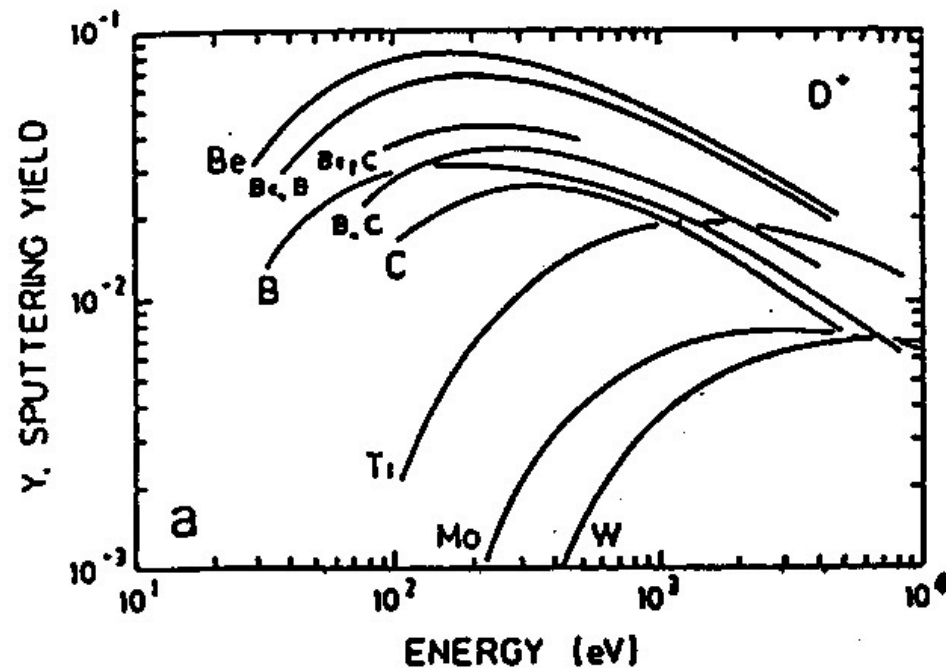
# Sputtering of PFC materials by particle flux

---

Large particle flux erodes PFC materials in the fusion reactor.

Small sputtering yield is desirable.

Lower plasma temperature makes the sputtering yield smaller.

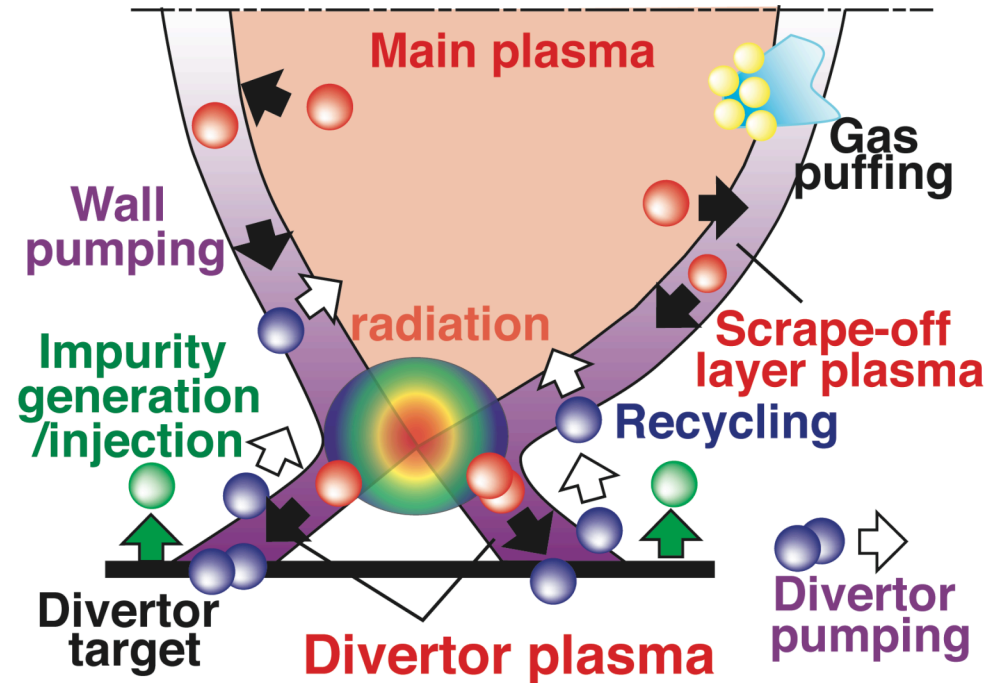


**How to achieve high radiative cooling and detachment of the divertor plasma in the fusion reactor?**



# Importance of Edge Plasma Simulation

- Understanding of Burning Plasma  
Complex system for SOL-divertor  
 $\rho^*, \beta, \nu^* + I_{A\&M-mfp}, L_{rad}(T_e)$
- Need of Numerical Simulation  
SOLPS, EDGE2D, UEDGE, SONIC, EMC3 etc
- Analysis/Prediction of Heat and Particle Control by Divertor  
Present devices,  
Future reactors (ITER, DEMO)



- Charged particle
- Recycling neutral
- Impurity
- Fuelled particle

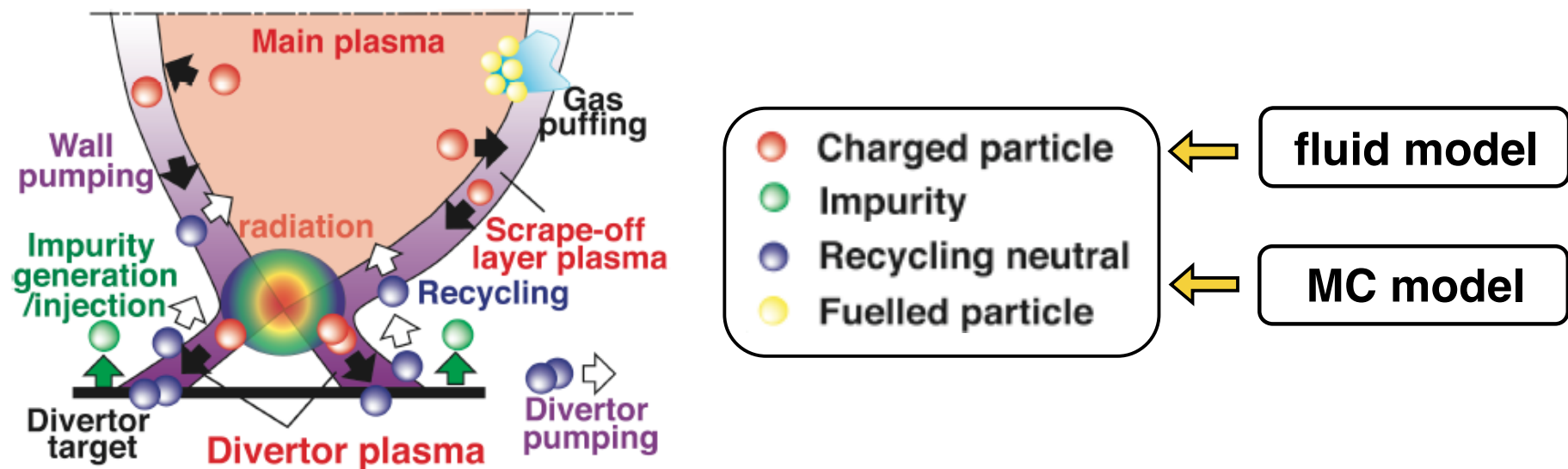
# Contents

1. Introduction : **Importance of Edge Plasma Simulation**
2. Multi-element Integrated SOL-Divertor Simulation  
: **Plasma fluid modeling and Neutral Monte Carlo modeling**
3. Coupling of Impurity Monte Carlo code
4. Further Integration of SONIC code
5. Physics Models for the Fluid Modeling
6. Particle Modeling  
: **Kinetic modeling for the verification of physics models**
7. PARASOL Simulation  
: **Kinetic modeling for the verification of physics models**

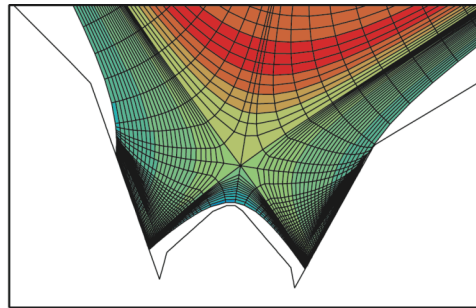
## Multi-element Integrated Simulation for SOL-divertor plasmas

SOLPS (B2/EIRENE), EDGE2D/NIMBUS,  
SONIC (SOLDOR/NEUT2D), EMC3/EIRENE etc,

where **plasma fluid equations** and  
**neutral-particle Monte-Carlo tracking** are coupled  
in the complex geometries of magnetic configuration and wall

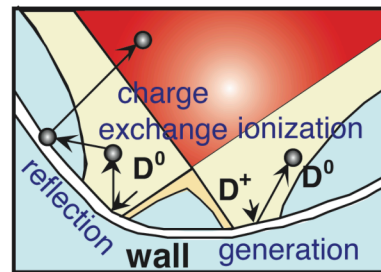


# 2. Multi-element Integrated SOL-Divertor Simulation

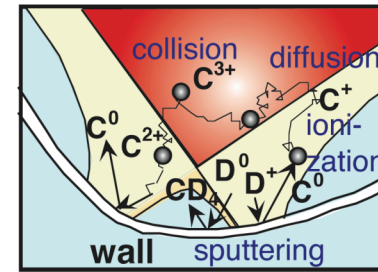
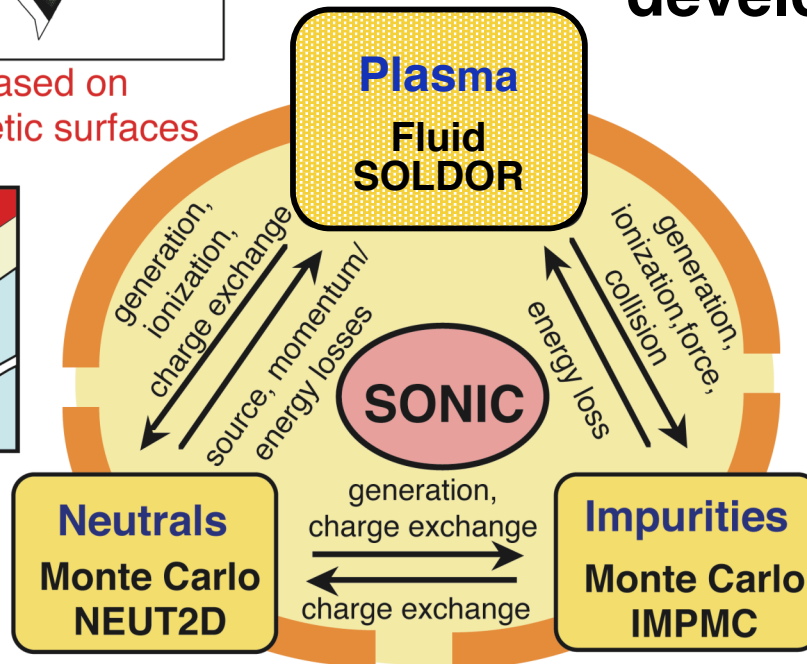


- Motions based on the magnetic surfaces

An example of integrated SOL-divertor code developed in JAEA



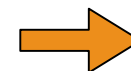
- Straight motion  
- Strong dependence on the wall structure



- Straight motion  
- Motions based on the magnetic surfaces

Plasma 2D Fluid Code  
Neutral MC Code  
Impurity MC Code

SOLDOR  
NEUT2D  
IMPMC



**SONIC**

H. Kawashima, K. Shimizu, T. Takizuka, et al., Plasma Fusion Res. 1 (2006) 031.

H. Kawashima, K. Shimizu, T. Takizuka, Plasma Phys. Control. Fusion 49 (2007) S77.

# Fluid equations for SOL-divertor plasma

---

Particle transport

$$\partial n / \partial t + \nabla_{\parallel} n V_{\parallel} + \nabla_{\perp} n \mathbf{v}_{\perp} = S \quad (\mathbf{v}_{\perp} \text{ consist of } \mathbf{v}_{\text{drift}}, v_{\text{pinch}}, \text{ and } -D \nabla_{\perp} \ln n)$$

Momentum transport

$$\partial m_i n V_{\parallel} / \partial t + \nabla_{\parallel} (m_i n V_{\parallel}^2 + p_i + p_e + \pi_i) + \nabla_{\perp} m_i n V_{\parallel} \mathbf{v}_{\perp} = S_M + \nabla_{\perp} n \chi_M \nabla_{\perp} V_{\parallel}$$

Ion energy transport

$$\begin{aligned} \partial \varepsilon_i / \partial t + \nabla_{\parallel} \left( \frac{1}{2} m_i n V_{\parallel}^2 + \frac{5}{2} p_i + \pi_i \right) V_{\parallel} + \nabla_{\perp} \varepsilon_i \mathbf{v}_{\perp} \\ = e n V_{\parallel} E_{\parallel} + Q_i + n (T_e - T_i) / \tau_{\text{eq}} + \nabla_{\parallel} \kappa_{i\parallel} \nabla_{\parallel} T_i + \nabla_{\perp} n \chi_i \nabla_{\perp} T_i \end{aligned}$$

Electron energy transport

$$\begin{aligned} \partial \varepsilon_e / \partial t + \nabla_{\parallel} \frac{5}{2} p_e V_{\parallel} + \nabla_{\perp} \varepsilon_e \mathbf{v}_{\perp} \\ = (j_{\parallel} - e n V_{\parallel}) E_{\parallel} + Q_e - n (T_e - T_e) / \tau_{\text{eq}} + \nabla_{\parallel} \kappa_{e\parallel} \nabla_{\parallel} T_e + \nabla_{\perp} n \chi_e \nabla_{\perp} T_e \end{aligned}$$

Ohm's law

$$E_{\parallel} = -(1/en) \nabla_{\parallel} p_e - (0.71/e) \nabla_{\parallel} T_e - Q_e / \sigma_{\parallel}$$

Current continuation

$$\nabla_{\parallel} j_{\parallel} + \nabla_{\perp} j_{\perp} = 0$$

## Simple steady-state solution for the 2D profile of $n$ and $V_{||}$

Particle balance equation and Momentum balance equation

$$\nabla_{||} n V_{||} - \nabla_{\perp} D \nabla_{\perp} n = 0 \quad , \quad \nabla_{||} (m_i n V_{||}^2 + p_i + p_e) = 0$$

Radial decay of  $n \sim \exp(-r/\lambda_n)$

$$\partial/\partial s (n V_{||}) - (D/\lambda_n^2) n = 0$$

Assume uniform temperature, and  $T_e + T_i = m_i C_s^2$

$$\partial/\partial s (V_{||}^2 + C_s^2) n = 0 \quad : \quad n = n(0) C_s^2 / (V_{||}^2 + C_s^2)$$

Particle balance equation becomes

$$\partial/\partial s \{ V_{||} / (V_{||}^2 + C_s^2) \} - (D/\lambda_n^2) / (V_{||}^2 + C_s^2) = 0$$

$$\{ -1 + 2C_s^2 / (V_{||}^2 + C_s^2) \} \partial V_{||} = (D/\lambda_n^2) \partial s$$

Parallel profile of  $V_{||}(s)$

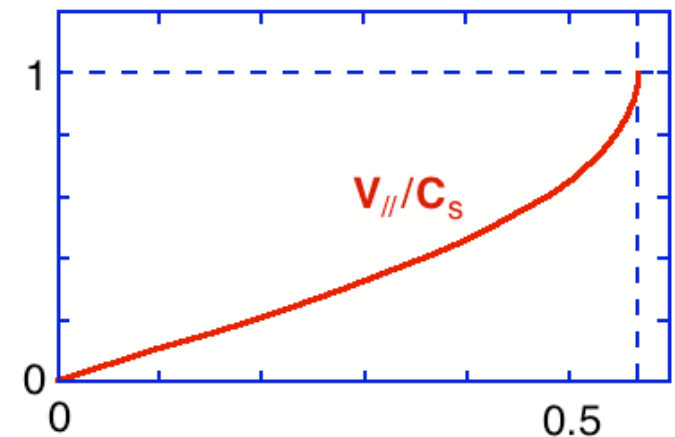
$$2 \tan^{-1} (V_{||} / C_s) - (V_{||} / C_s) = (D/\lambda_n^2 C_s) s$$

Boundary condition for  $V_{||}$  at the divertor plate  $s = L$ ,

$V_{||} = C_s$ , gives the density decay length  $\lambda_n$

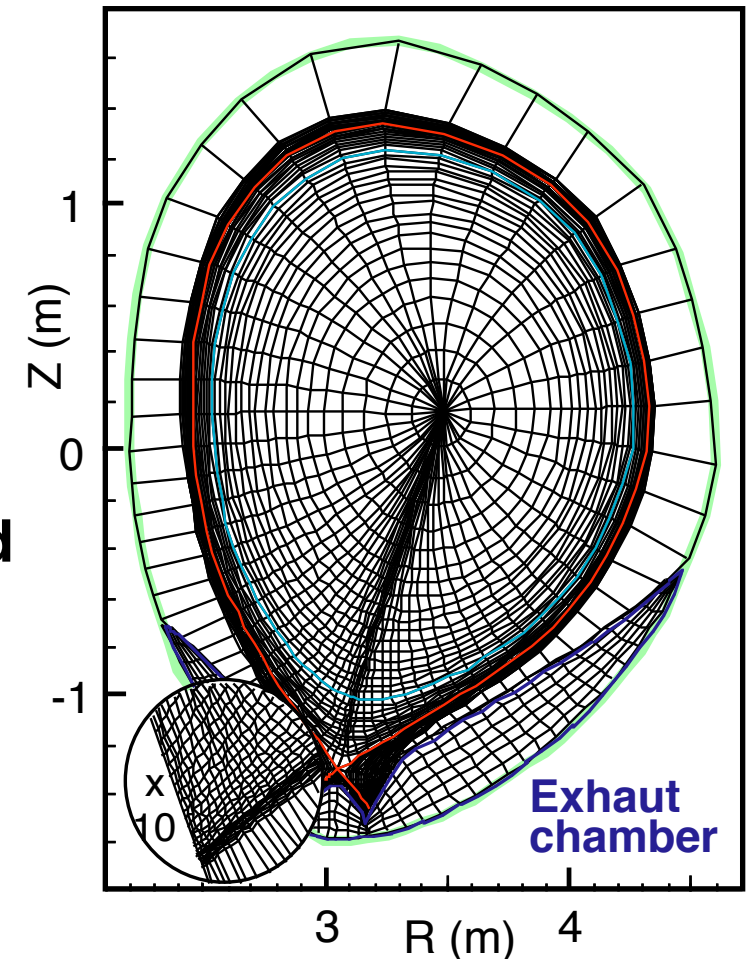
$$\lambda_n = (DL/0.57 C_s)^{1/2}$$

$ex. T = 100 \text{ eV}, D = 0.5 \text{ m}^2/\text{s}, L = 100 \text{ m} : \lambda_n = 3 \text{ cm}$



# SOLDOR code

- **2D Plasma Fluid modeling (w/o impurity)**
    - **Complex divertor geometry**
      - Finite volume method
      - Boundary-fitted grids
      - Fine meshes near divertor plate ( $\leq 2\text{mm}$ )
    - **Strong nonlinearity of equations**
      - Linearization by Newton-Raphson method
    - **2D finite difference equations**
      - Approximate factorization method
    - **Numerical stability for convective terms**
      - Total variation-diminishing scheme
- small numerical diffusion



**JT-60U W-shaped divertor**

$$N_{\psi} = 37 \quad (r/a > 0.95)$$

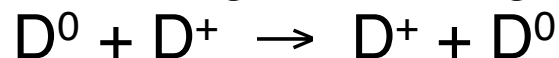
$$N_{\chi} = 120$$

# Monte Carlo model for neutral particles

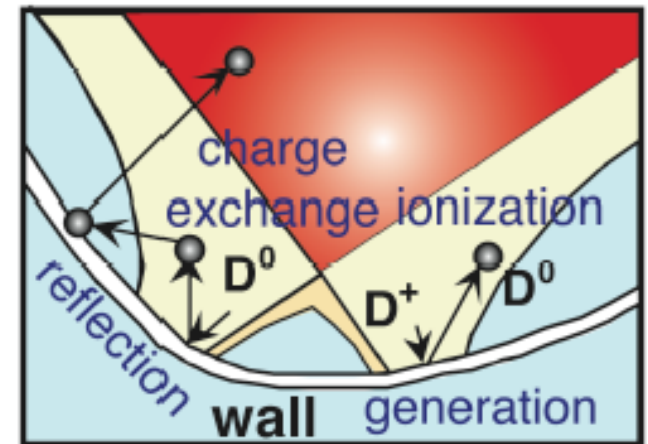
- **Accurate and easy modeling of A&M processes**
- **Accurate and easy treatment of vacuum region/pumping room**

Test neutral particle  $D^0$  with a velocity  $\mathbf{v}(t=0)$

If  $\xi < v_{cx} \Delta t$  (uniform random number  $0 < \xi < 1$ ),  
then a charge exchange occurs



Random generation of  $\mathbf{v}(t=\Delta t)$  from  
a shifted Maxwell distribution of the ion



## Reduction of MC noise in **NEUT2D** code

( larger MC noise due to small test particle number  
in smaller mesh volume near the plates )

- **“Piling method” ; efficient time average**
- **Massive parallel computation ; lots of test particles**



### 3. Coupling of Impurity Monte Carlo Code

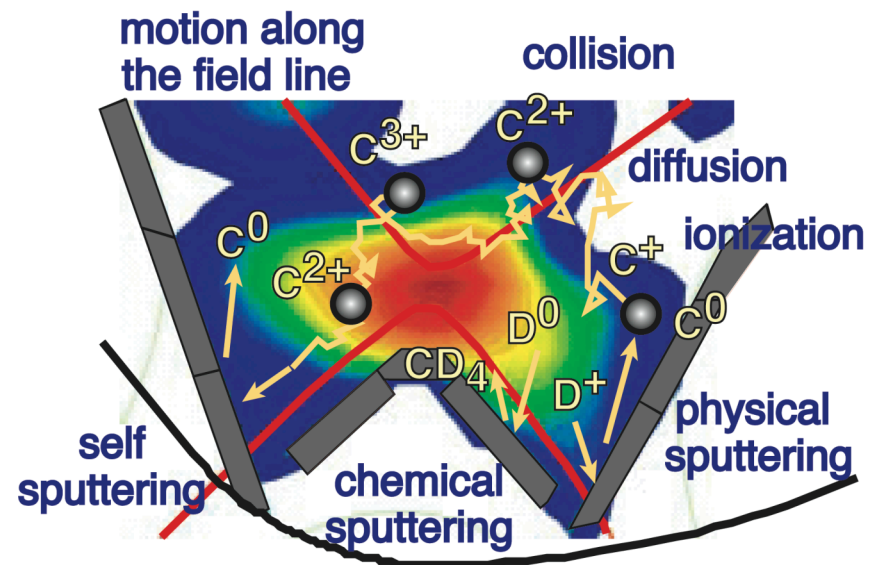
Majority of integrated divertor codes employ fluid modeling for impurities, while **SONIC** employs Monte Carlo modeling;

**SONIC** : SOLDOR/NEUT2D/IMPMP

**IMPMP** : IMPurity Monte-Carlo code

The MC approach is very suitable for the modeling of

- impurity generation
- kinetic effects including various collisional effects
- interaction between impurity and wall
- complicated dissociation processes of methane ( $\text{CD}_4$ )



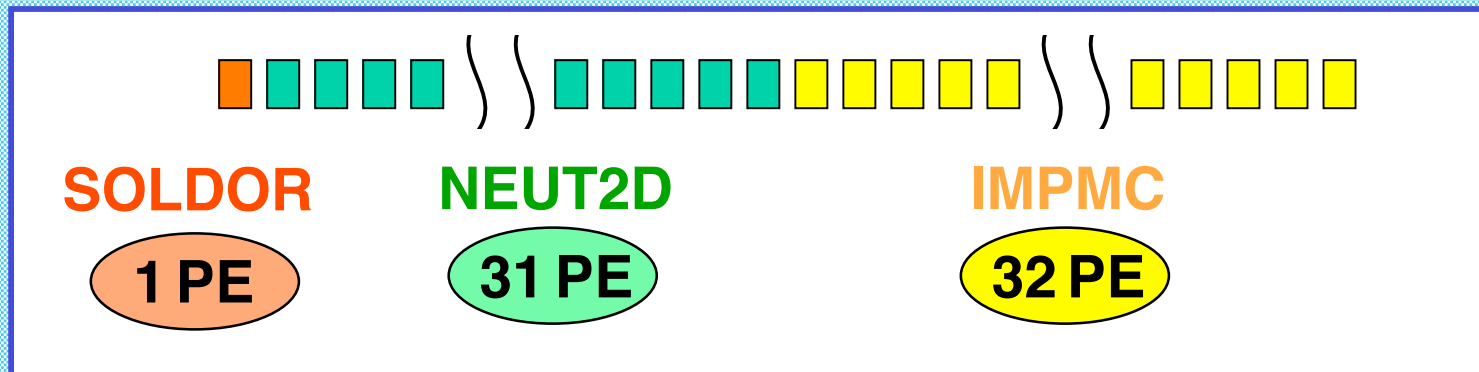
The MC approach, however, is disadvantageous for

- **long computational time due to very short time step**
- **large MC noise due to restricted test particle number**
- **increasing large particle number in time-dependent simulation**

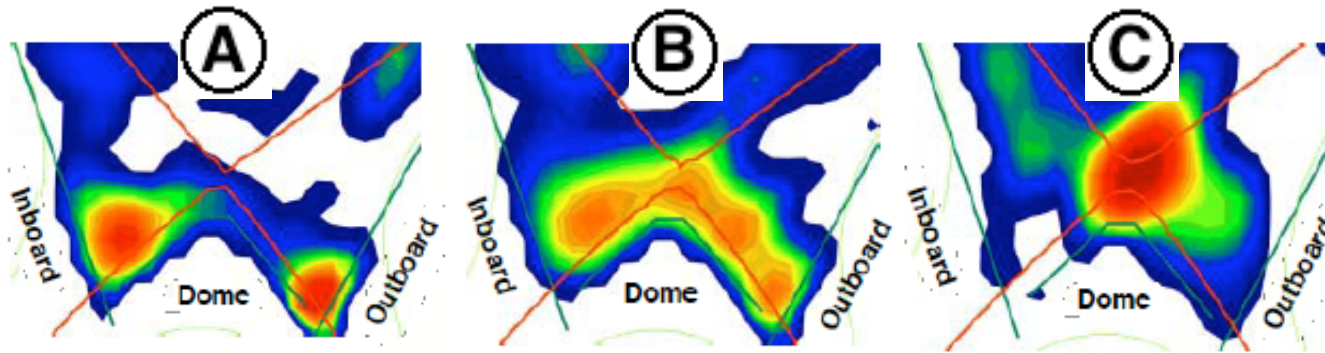
We have solve these problems with

- **new diffusion model for a scattering process**
- **optimization on a massive parallel computer**
- **particle reduction scheme**

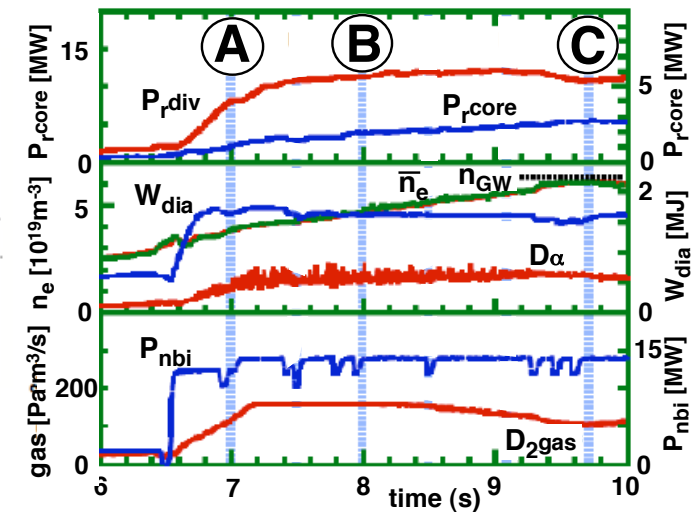
### Optimization of SONIC on a massive parallel computer



# Time evolution of radiation distribution in JT-60U

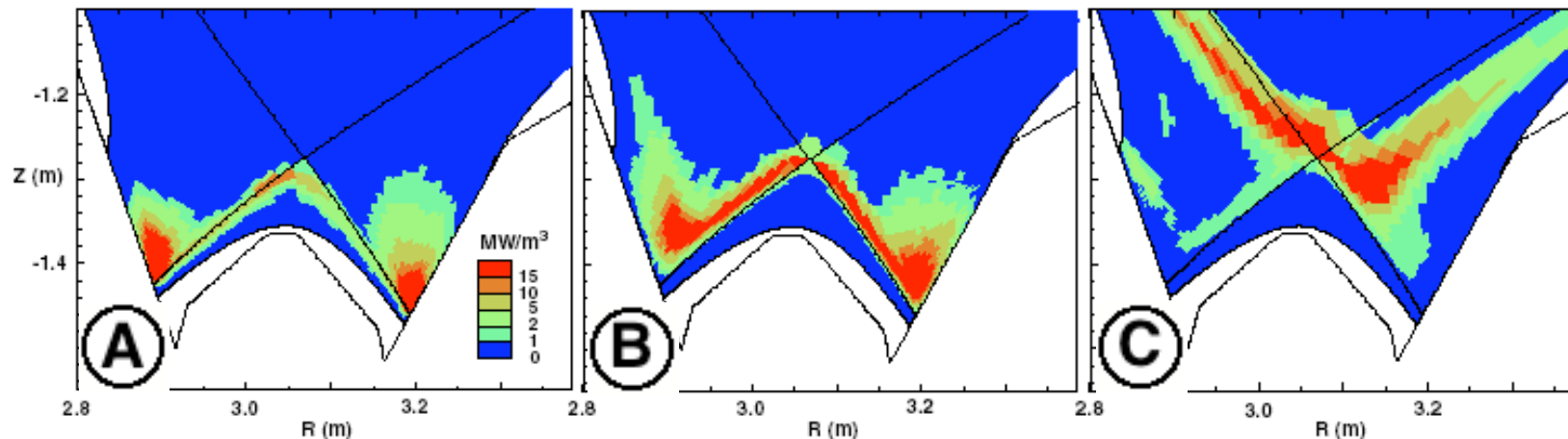


S. Konoshima et al. J. Nucl. Mater. **313-316** (2003) 882.



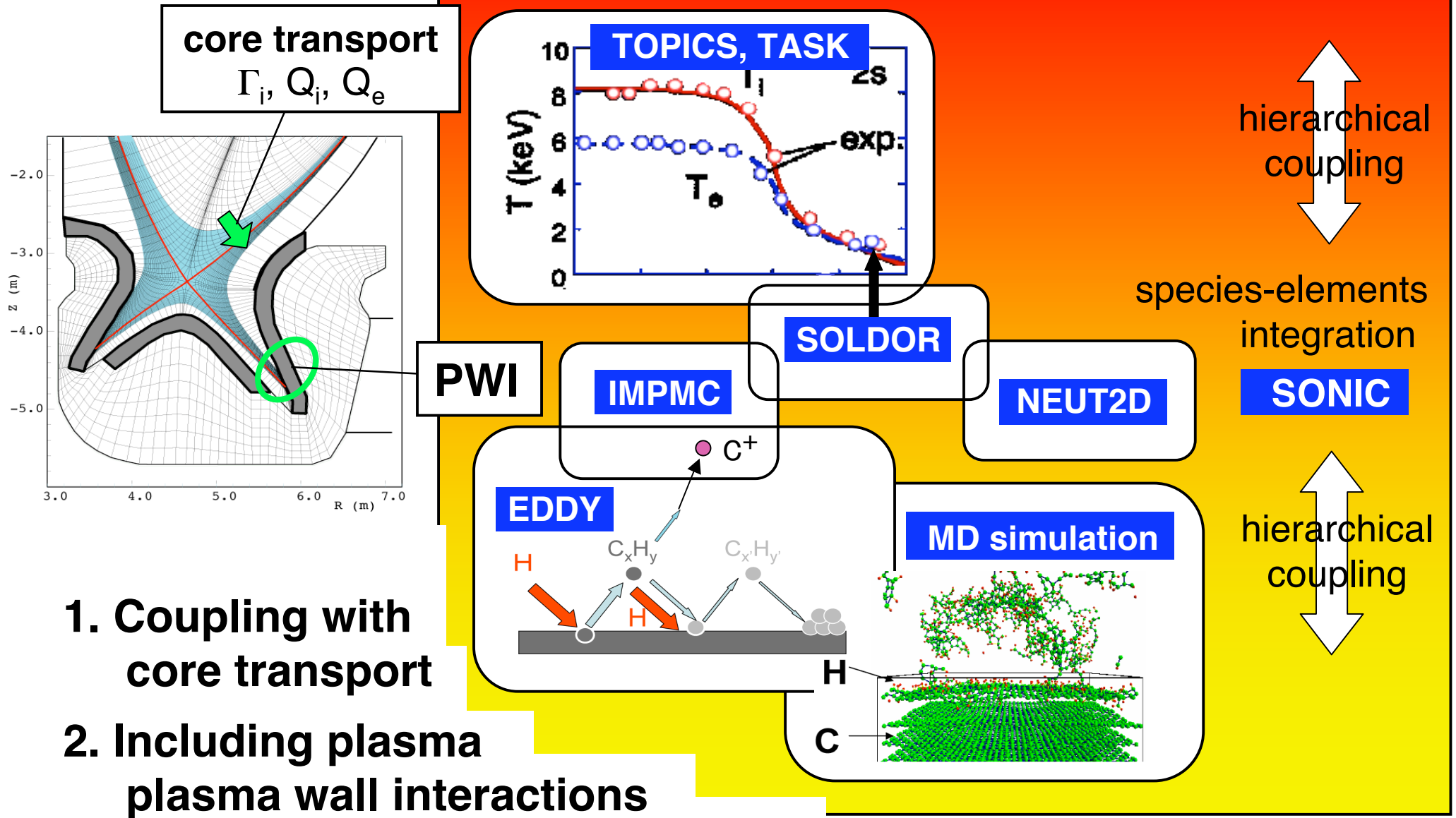
**SONIC simulation reproduced fairly well the evolution of the radiation.**

In the detached plasma, a part of carbons sputtered from the dome penetrate directly into the main plasma and contribute to the X-point MARFE.



K. Shimizu<sup>1</sup>, T. Takizuka<sup>1</sup>, et al., Nucl. Fusion **49** (2009) 065028.

# 4. Further Integration of SONIC Code – Hierarchical coupling –



1. Coupling with core transport
2. Including plasma plasma wall interactions

## 5. Physics Models for the Fluid Modeling

**Various physics models** in fluid modeling for SOL-divertor plasmas;

boundary condition  $V_{//} = C_s$  (Bohm criterion)

heat conductivity  $q_{\text{cond}} = -\kappa_{//} \nabla_{//} T$  etc

Boundary condition for  $V_{//}$  at the divertor plate  $s = L$ ,  $V_{//} = C_s$ ,  
gives the density decay length  $\lambda_n = (DL/0.57C_s)^{1/2}$ .

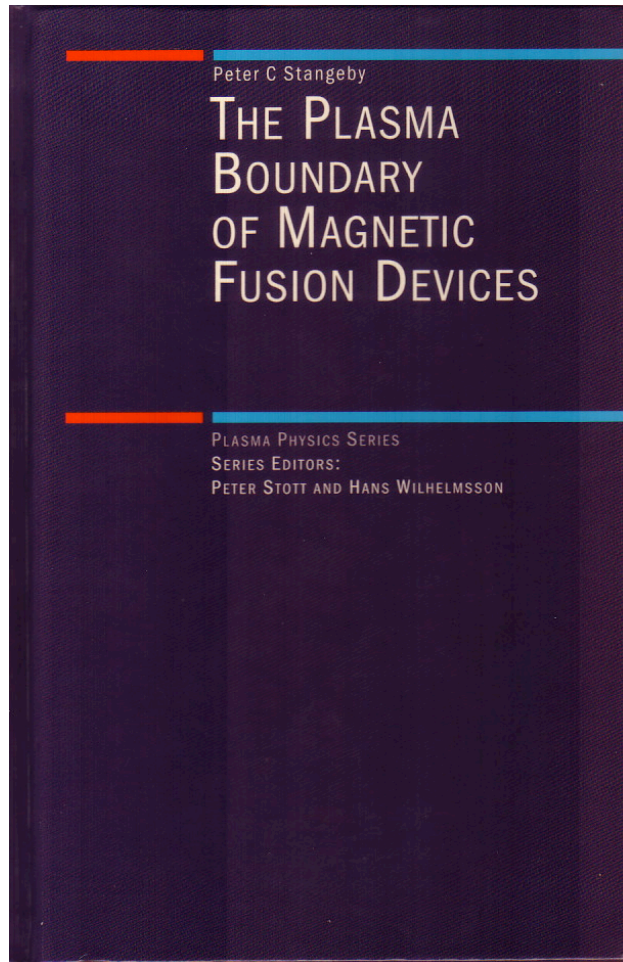
Density at the separatrix  $n_{\text{sep}}$  is determined from the particle flux

$$\Gamma_{\perp} = Dn_{\text{sep}} S_{\text{sep}} / \lambda_n ; n_{\text{sep}} = (L/0.57DC_s)^{1/2} \Gamma_{\perp} / S_{\text{sep}} .$$

**In other words, the value of  $n_{\text{sep}}$  cannot be determined without giving a boundary condition of  $V_{//}$  under the fluid modeling .**



# Fundamental Physics of “THE PLASMA BOUNDARY OF MAGNETIC FUSION DEVICES” is found in a text book by P.C. Stangeby (Taylor & Francis, New York)



Part 1 An introduction to the subject of the plasma boundary  
Simple Analytic Models of the Scrape-Off Layer  
The Role and Properties of the Sheath  
Experimental Databases Relevant to Edge Physics  
Simple SOL, The Divertor SOL, Plasma Impurities  
The H-Mode and ELM, Fluctuation in the Edge Plasma

PART 2 Introduction to fluid modelling of the boundary plasma  
The 1D Fluid Equations  
1D Models for the Sheath-Limited SOL  
1D Modelling of the Conduction-Limited SOL  
'Onion-Skin' Method for Modelling the SOL  
An Introduction to Standard 2D Fluid Modelling of the SOL

PART 3 Plasma Boundary Research  
Supersonic Flow, Flow Reversal, Divertor Detachment,  
Current in the SOL, Drift, Density,  $\chi_{\perp}$ ,  $D_{\perp}$ , MARFES,  
Radiating Plasma Mantle,  $Z_{\text{eff}}$ ,  $P_{\text{rad}}$ , Sheath,  
Kinetic Effects, Impurity Injection

## Bohm criterion for sheath formation

– Ion flow speed at the plasma-sheath boundary –

### Stable (exponential type) solution of Poisson's equation

Electron  $0 = -d(n_e T_e)/dx + e n_e d\phi/dx : n_e = n_0 \exp(e\phi/T_e)$

Ion  $m_i n_i V dV/dx = -d(n_i T_i)/dx - e n_i d\phi/dx, \delta(n_i T_i)/(n_i T_i) = \gamma_a \delta n_i/n_i$   
 $d(n_i V)/dx = 0 : (m_i V_0^2 - \gamma_a T_i) dn_i/dx = e n_0 d\phi/dx$

Poisson's equation  $-d^2\phi/dx^2 = e/\epsilon_0 (n_i - n_e)$

$$e\phi/T_e = \Phi, \delta n_i/n_0 = \Phi T_e/(m_i V_0^2 - \gamma_a T_i), \delta n_e/n_0 = -\Phi, X = x/\lambda_D, \lambda_D^2 = e^2 n_0/\epsilon_0 T_e$$

$$-d^2\Phi/dX^2 = \{T_e/(m_i V_0^2 - \gamma_a T_i) - 1\} \Phi$$

$$k^2 \equiv 1 - T_e/(m_i V_0^2 - \gamma_a T_i) \geq 0 : \Phi \sim \exp(kX)$$

$$k_*^2 \equiv T_e/(m_i V_0^2 - \gamma_a T_i) - 1 \geq 0 : \Phi \sim \cos(k_* X) \text{ unstable (oscillatory)}$$

solution

Stable solution  $k^2 \geq 0 : m_i V_0^2 \geq T_e + \gamma_a T_i$  **Bohm criterion**

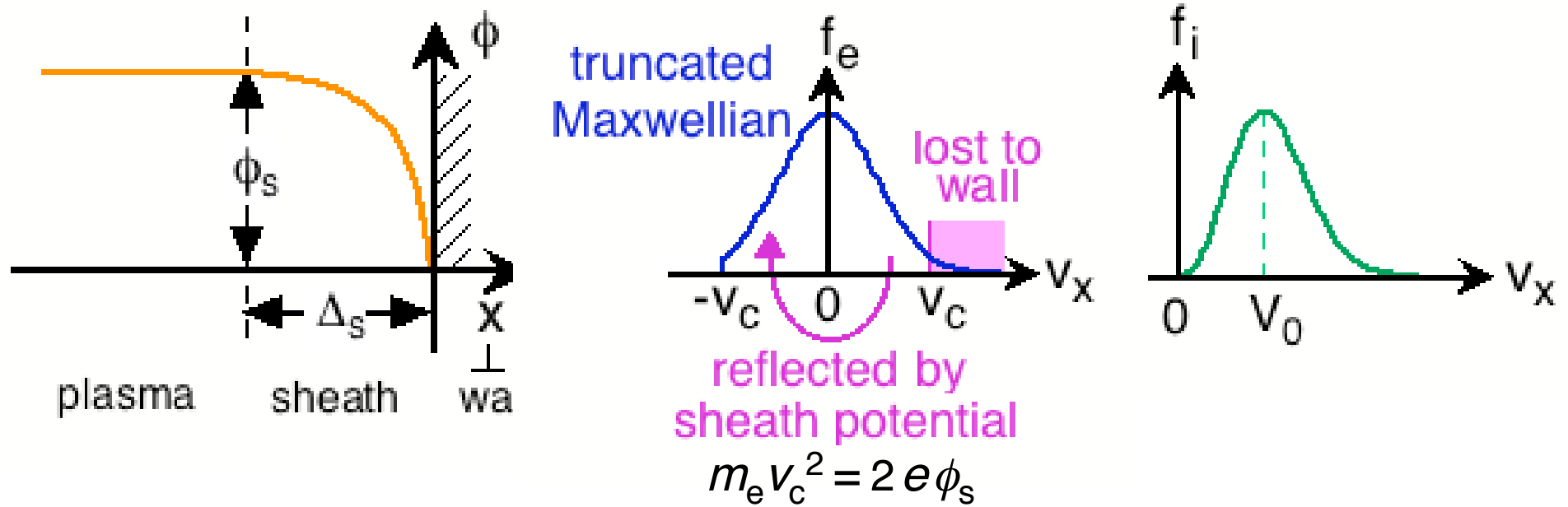
## Sheath potential to keep charge neutrality

Electrons run off to the end plate faster than ions.

Electrostatic potential grows by positive charging in front of the plate.

Electrons are reflected by this sheath potential.

Electrons and ions flow into the plate equally, in steady state.



$$V_0 = \int v f_e dv \equiv (2\pi m_e / T_e)^{1/2} \int_{-v_c}^{\infty} v \exp(-m_e v^2 / T_e) dv = (2\pi T_e / m_e)^{1/2} \exp(-m_e v_c^2 / T_e)$$

$$e \phi_s / T_e = \frac{1}{2} \ln(m_i / 2\pi m_e) - \frac{1}{2} \ln(m_i V_0^2 / T_e)$$



## 6. Particle Modeling

**Various physics models** (e.g., boundary condition  $V_{||} = C_s$ ) are employed in the **fluid modeling** for SOL-divertor plasmas.

**Kinetic approach** is necessary to validate such physics models.

One of the most powerful kinetic models is **particle simulation** (full  $f$  or  $\delta f$ , full motion or gyrokinetic).

cf. **continuum modeling**

$$\partial f / \partial t + \mathbf{v} \cdot \nabla_{\mathbf{r}} f + (q\mathbf{E} + \mathbf{v} \times \mathbf{B}) \cdot \nabla_{\mathbf{v}} f = C(f, f) + S$$

R. Cohen, X.Q. Xu, Contrib. Plasma Phys. **48** (2008) 212.

C.K. Birdsall, IEEE Trans. Plasma Sci. **19** (1991) 65.

J.P. Verboncoeur, Plasma Phys. Control. Fusion **47** (2005) A231.

**PARASOL code has been developed for studying the physics of SOL and divertor plasmas.**

**( PARTicle Advanced simulation for SOL and divertor plasmas )**

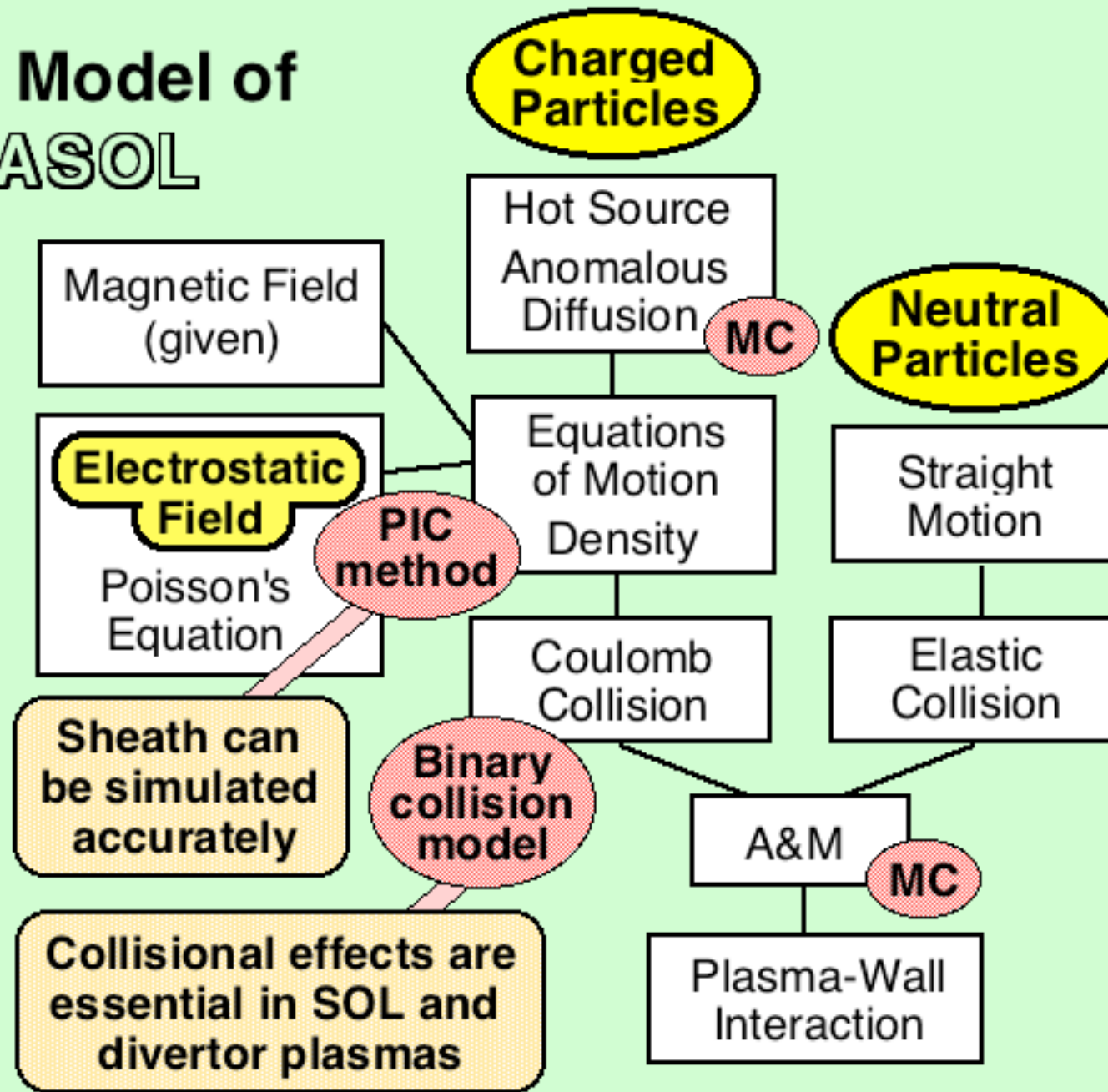
T. Takizuka et al., proc. 8th IAEA Conf., Brussels 1980, **Vol. 1** (1981) p.679.

R. Chodura, Phys. Fluids **25** (1982) 1628.

T. Takizuka et al., J. Nucl. Mater. **128-129** (1984) 104.

T. Takizuka, M. Hosokawa, Contrib. Plasma Phys. **40** (2000) 471.

# Physics Model of PARASOL



T. Takizuka, M. Hosokawa, K. Shimizu, Trans. Fusion Technol. **39** (2001) 111.  
 T. Takizuka, M. Hosokawa, K. Shimizu, J. Nucl. Mater. **313-316** (2003) 1331.

# Particle Motion

---

## Collisionless motion of an ion

$$m_i \, d\mathbf{v}/dt = e (\mathbf{E} + \mathbf{v} \times \mathbf{B}) + \mathbf{F}_c$$

$$d\mathbf{r}/dt = \mathbf{v}$$

centrifugal force  $\mathbf{F}_c = m_i (v_\theta^2/R, -v_R v_\theta/R, 0)$

in the cylindrical coordinates  $(R, \theta, Z)$  and  $(v_R, v_\theta, v_Z)$

## Collisionless motion of an electron guiding-center

$$m_e \, dv_{//}/dt = -e \mathbf{E} \cdot \mathbf{B}/B - \mu \nabla_{//} B + m_e v_{//} \mathbf{v}_{E \times B} \cdot \nabla B/B$$

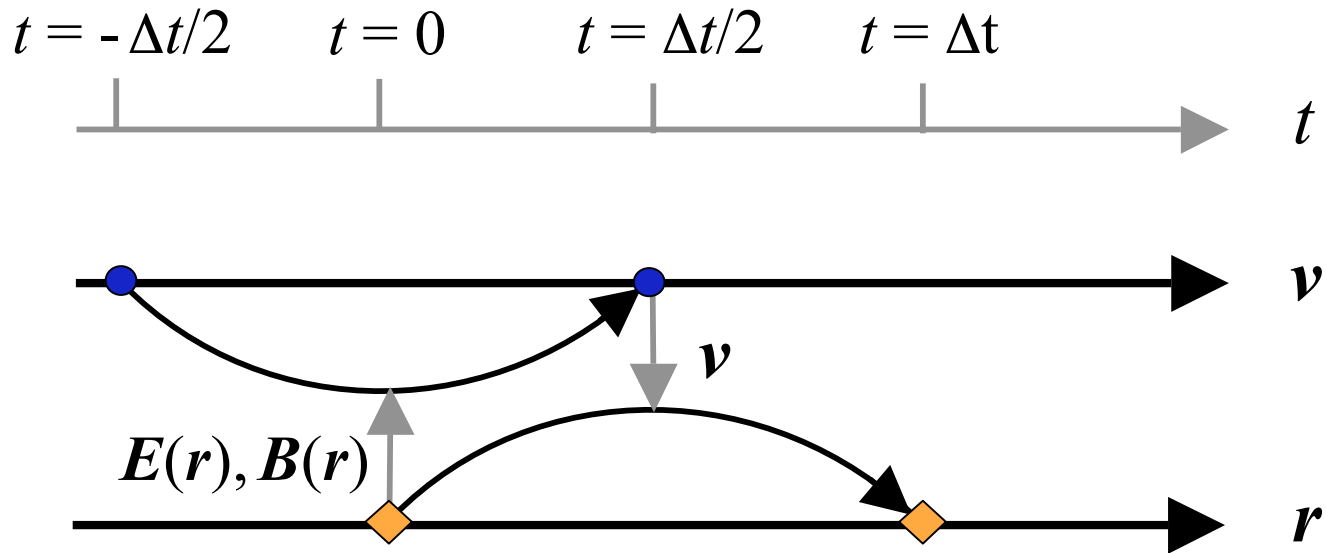
$$d\mathbf{r}/dt = v_{//} \mathbf{B}/B + \mathbf{v}_{E \times B} + \mathbf{v}_{\nabla B}$$

magnetic moment  $\mu \equiv m_e v_\perp^2/2B = \text{const.}$

$\mathbf{E} \times \mathbf{B}$  drift  $\mathbf{v}_{E \times B} = (\mathbf{E} \times \mathbf{B})/B^2$

curvature drift  $\mathbf{v}_{\nabla B} = (-m_e/2eB^3) (2v_{//}^2 + v_\perp^2) (\nabla B \times \mathbf{B})$

# Leap-frog method for the equation of ion motion



$$m_i (\mathbf{v}^{\Delta t/2} - \mathbf{v}^{-\Delta t/2}) / \Delta t = e (\mathbf{E}(\mathbf{r}^0) + \frac{1}{2} (\mathbf{v}^{\Delta t/2} + \mathbf{v}^{-\Delta t/2}) \times \mathbf{B}(\mathbf{r}^0)) + \mathbf{F}_c$$

$$(\mathbf{r}^{\Delta t} - \mathbf{r}^0) / \Delta t = \mathbf{v}^{\Delta t/2}$$

$$F_{c,R} = m_i (v_{\theta}^{\Delta t/2} + v_{\theta}^{-\Delta t/2}) v_{\theta}^{-\Delta t/2} / 2R^0$$

$$F_{c,\theta} = -m_i (v_R^{\Delta t/2} + v_R^{-\Delta t/2}) v_{\theta}^{-\Delta t/2} / 2R^0$$

Linearized centrifugal force  
(Energy conservation)

## Gyro motion followed by leap-frog method

$$m_i (\mathbf{v}^{\Delta t/2} - \mathbf{v}^{-\Delta t/2}) / \Delta t = e \frac{1}{2} (\mathbf{v}^{\Delta t/2} + \mathbf{v}^{-\Delta t/2}) \times \mathbf{B}(r^0)$$

### Energy conservation

$$\begin{aligned} (\mathbf{v}_+ - \mathbf{v}_-) \cdot (\mathbf{v}_+ + \mathbf{v}_-) &= (e\Delta t/2m_i) \{ (\mathbf{v}_+ + \mathbf{v}_-) \times \mathbf{B} \} \cdot (\mathbf{v}_+ + \mathbf{v}_-) \\ (\mathbf{v}_+)^2 - (\mathbf{v}_-)^2 &= 0 \end{aligned}$$

### Small phase delay without numerical drift

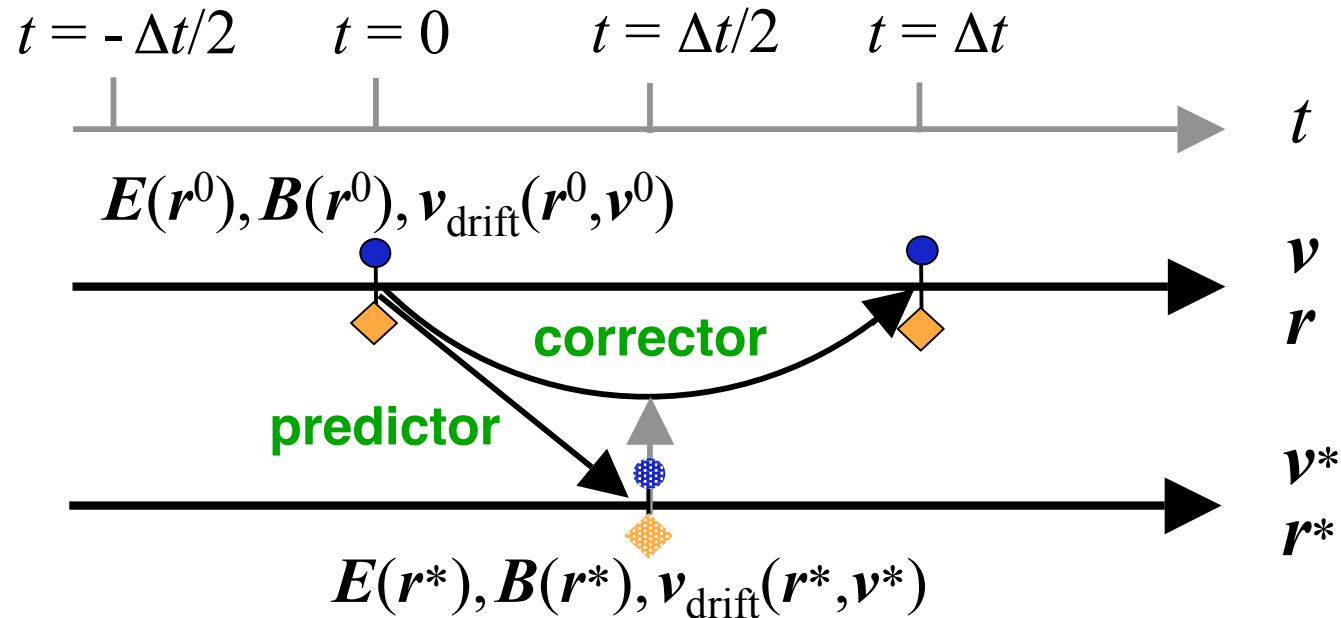
$$V_+ - V_- = (h/2)(U_+ + U_-), \quad U_+ - U_- = -(h/2)(V_+ + V_-) \quad (h \equiv \Omega \Delta t)$$

$$V_+ = \sin \theta_+, \quad V_- = \sin \theta_-, \quad U_+ = \cos \theta_+, \quad U_- = \cos \theta_-$$

$$\sin \frac{1}{2}(\theta_+ - \theta_-) = (h/2) \cos \frac{1}{2}(\theta_+ - \theta_-)$$

$$\theta_+ - \theta_- = 2 \tan^{-1}(h/2) \approx \Omega \Delta t \left( 1 - \frac{1}{12} h^2 \right)$$

## Predictor-corrector method for the equation of electron guiding center



$$m_e \, dv_{\parallel}/dt = -e \, \mathbf{E} \cdot \mathbf{B}/B - \mu \, \nabla_{\parallel} B + m_e \, v_{\parallel} \, \mathbf{v}_{\text{ExB}} \cdot \nabla B/B$$

$$dr/dt = v_{\parallel} \, \mathbf{B}/B + \mathbf{v}_{\text{ExB}} + \mathbf{v}_{\nabla B}$$

It is necessary to solve Poisson's equation at  $t=0$  (predictor step) and at  $t=\Delta t/2$  (corrector step), respectively.

Positions of ions,  $r^*$  at  $t=\Delta t/2$ , are to be solved.

# Anomalous Diffusion

---

## Monte-Carlo random-walk model

Spatial displacement  $\Delta \mathbf{r}_{\text{anom}}$  given by Gaussian random number

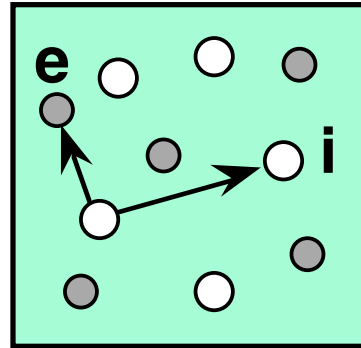
$$\langle \Delta \mathbf{r}_{\text{anom}} \rangle = 0, \quad \langle \Delta \mathbf{r}_{\text{anom}}^2 \rangle = 2 D_{\text{anom}} \Delta t$$

Ambipolar diffusion,  $\Gamma_i = \Gamma_e$ , is maintained when  $D_{\text{anom}}$  is uniform and constant for all ion and electron particles.

Diffusion displacement at  $t = \Delta t/2$  (corrector step) is simply approximated as  $\Delta \mathbf{r}_{\text{anom}}(\Delta t/2) = \frac{1}{2} \Delta \mathbf{r}_{\text{anom}}(\Delta t)$ .

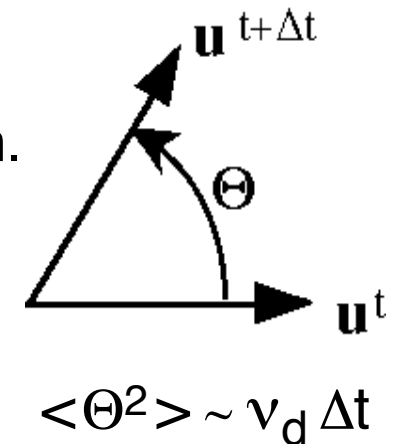
# Coulomb Collisions - Binary collision model -

(1) In a time interval, a particle in a cell suffers binary collisions with an ion and an electron which are chosen randomly in the same cell.



(2) Change in the relative velocity results from a coulomb interaction.

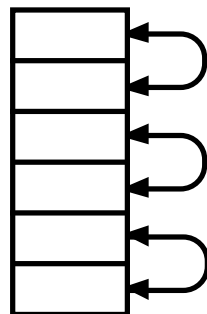
Total momentum and total energy are conserved intrinsically.



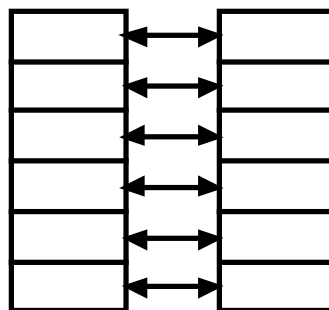
## Random selection of collision pairs

At first; random rearrangement of addresses in every cell at every time step.

Next ;



like-particles



ion-electron

## Landau collision integral

T. Takizuka, H. Abe, J. Comput. Phys. **25** (1977) 205.



# Electric field - PIC method -

---

## Poisson's equation and electrostatic field

$$-\nabla^2\phi = (e/\varepsilon_0)(n_i - n_e) \quad E_s = -\nabla\phi$$

Density ( $n_i$  and  $n_e$ ) is calculated with a PIC method of the area-weighting scheme.

Density is assigned in inverse-proportion to the particle radial position,  $1/R$ , for the cylindrical coordinates.

## Boundary condition

1D PARASOL : divertor plates at both sides

(1) biasing  $\phi(-L/2) = 0$  and  $\phi(L/2) = \Delta\phi$

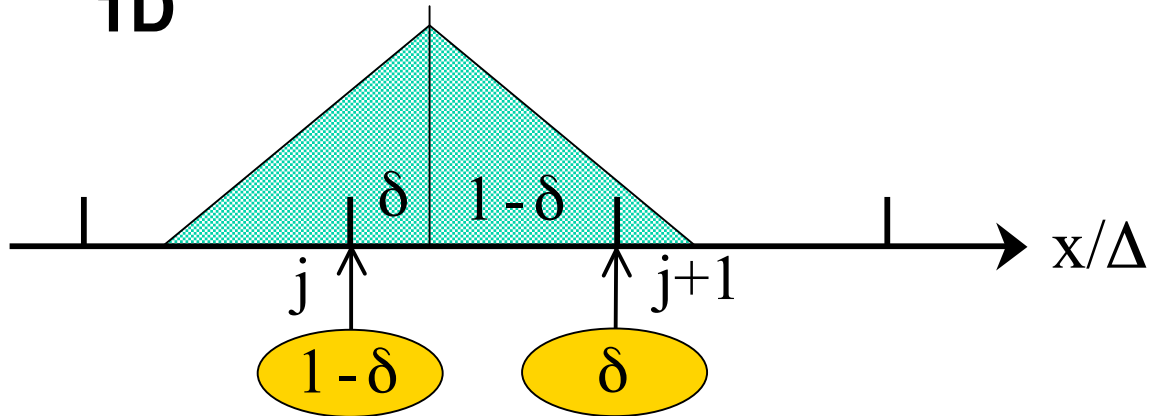
(2) current control  $\Delta\phi = G \int dt (I - I_{set})$

2D toroidal PARASOL : surrounded by the rectangular walls

(1) conducting wall  $\phi = 0$  on the rectangular walls

# PIC method of the area-weighting scheme

1D



$$n_j = \sum (1-\delta)$$

$$n_{j+1} = \sum \delta$$

$\Sigma$  for particles

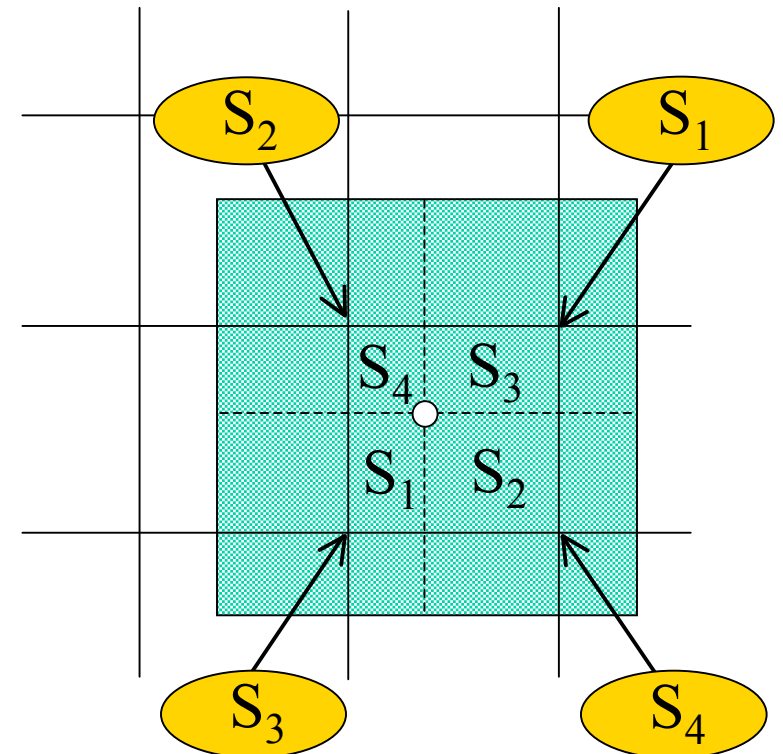
$$E = (1-\delta)E_j + \delta E_{j+1}$$

for each particle

Poisson's eq.  $\phi_j$

$$E_j = (\phi_{j-1} - \phi_{j+1})/2\Delta$$

2D



# Poisson Solver

**Tri-diagonal Matrix Algorithm in the  $R$  direction**  
**Fast Fourier Transform algorithm in the  $Z$  direction**

$$-\nabla^2\phi = (e/\epsilon_0)(n_i - n_e)$$

## 1D difference equation

$$(\phi_{j+1} - 2\phi_j + \phi_{j-1})/\Delta^2 = -\rho_j$$

**cylindrical coordinates  $(R, \theta, Z)$   $\nabla^2\phi \rightarrow R^{-1}\partial/\partial R(R\partial/\partial R)$**

$$(R_{j+1/2}\phi_{j+1} - 2R_j\phi_j + R_{j-1/2}\phi_{j-1})/R_j\Delta^2 = -\rho_j$$

## 1D difference equation (Fourier expansion in $k$ direction)

$$(\phi_{j+1} - 2\phi_j + \phi_{j-1})_k/\Delta^2 + (\phi_{k+1} - 2\phi_k + \phi_{k-1})_j/\Delta^2 = -\rho_{j,k}$$

$$(\phi_{j+1} - 2\phi_j + \phi_{j-1})_m/\Delta^2 - (2\pi m^*/L)^2\phi_{j,m} = -\rho_{j,m}$$

$$m_*^2 = 2(1 - \cos 2\pi m\Delta/L)/(2\pi\Delta/L)^2 \approx m^2 \{ 1 - (2\pi m\Delta/L)^2/12 \}$$

# System size

Fusion plasma  $L/\lambda_D > 10^4$  / PARASOL plasma  $L/\lambda_D < 10^3$

System size  $L$ , Mesh size  $\Delta \sim \lambda_D$

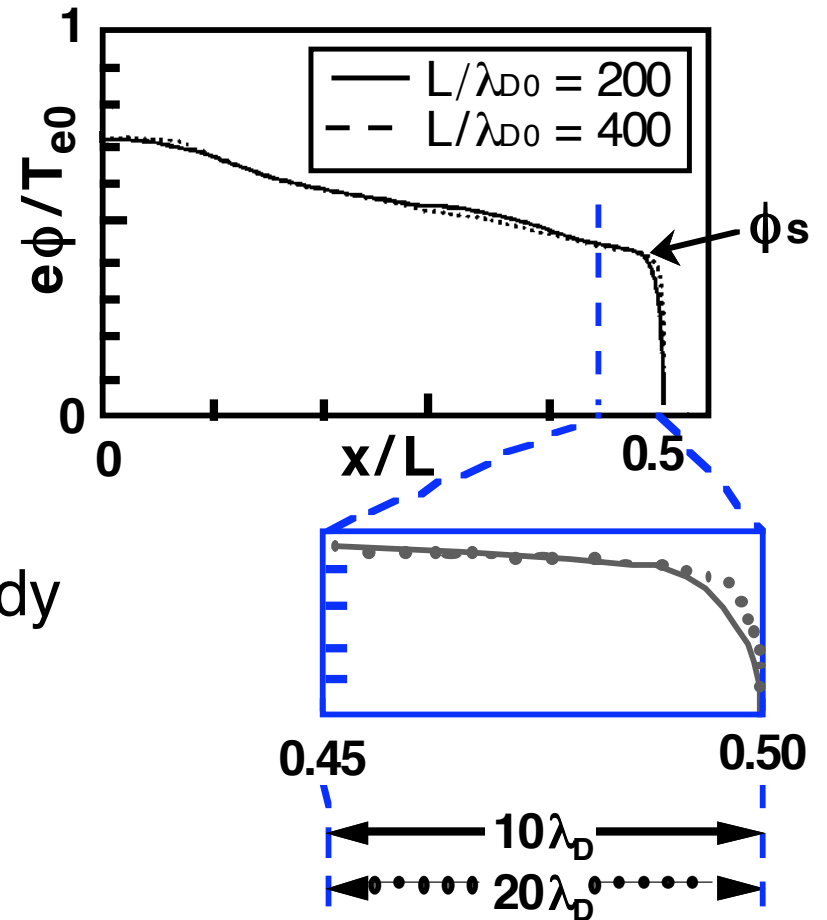
Particle number  $N \propto (L/\lambda_D)^{1,2,3} \leftarrow$  dimension

Characteristic time for equilibrium  $L/C_s$

Time steps  $K_t \propto (m_i/m_e)^{1/2} (L/\lambda_D)$

Computation time  $t_c \propto (m_i/m_e)^{1/2} (L/\lambda_D)^{2,3,4}$

**PARASOL** simulations are available to study open-field plasmas with smaller values of  $L/\lambda_D \sim 10^{2-3}$ , because characteristics are almost unchanged by changing  $L/\lambda_D$  value except the sheath region.



By introducing the binary collision model, we can flexibly perform **PARASOL** simulations at any **arbitrary collisionality**  $L_{//}/l_{mfp}$

# Source, Heating, Cooling etc.

---

## Hot particle source :

Diffusive flux from core to **1D** SOL central region

Beam supply to **2D** core region *a)* artificial beam with temperature  $T_0$   
*b)* realistic beam with energy  $E_b$

**Cold source** : recycling near the plate  
gas puff fueling

**RF heating** and **Alpha heating** in the core region

**Radiative cooling** in the divertor region

**Momentum loss** due to charge-exchange in the divertor region

**Supplied particles are finally lost to the wall.  
Supply and loss are balanced in the steady state.**

# Advancing time steps

## (SOURCE)

$r(0)$  &  $v(0)$  at  $t=0$

## Density

$n_e$  &  $n_i$  for  $r(0)$

## Poisson's eq.

$E$  at  $t=0$

## Particle motion

$r^*_0(\Delta t/2)$   
 $v^*_0(\Delta t/2)$

## Diffusion

$$r^* = r^*_0 + \frac{1}{2} \Delta r_{\text{anom}}$$

## Density

$n_e$  &  $n_i$  for  $r^*$

## Poisson's eq.

$E^*$  at  $t=\Delta t/2$

## Particle motion

$r_0(\Delta t)$   
 $v_0(\Delta t)$

## Diffusion

$$r(\Delta t) = r_0(\Delta t) + \Delta r_{\text{anom}}$$

## Collision

$$v(\Delta t) = v_0(\Delta t) + \Delta v_{\text{col}}$$

## Heating, Cooling and Charge exchange

$v(\Delta t) \Rightarrow v'(\Delta t)$

YES

NO

## Loss to the wall

**SOURCE**

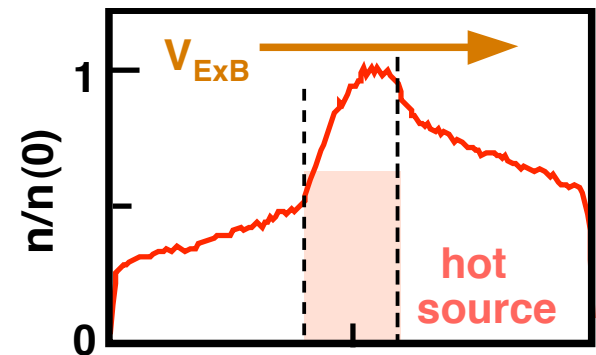
$r(\Delta t)$  &  $v(\Delta t) \Rightarrow r(0)$  &  $v(0)$

# 7. PARASOL Simulation

## Verification of the Bohm criterion

### 1D PARASOL simulation

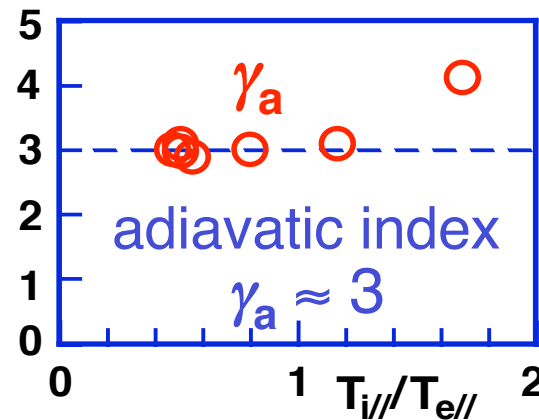
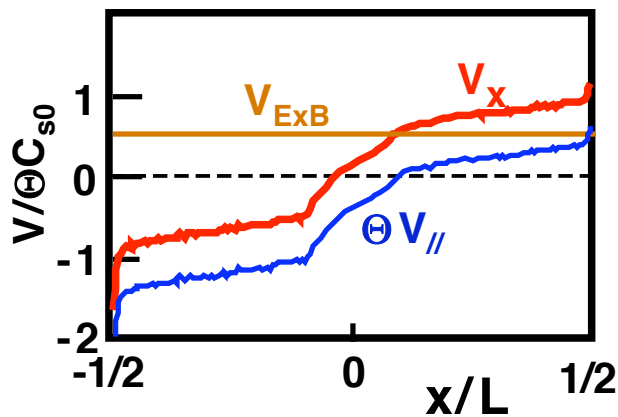
Oblique  $\mathbf{B}$  ( $\Theta = B_x/B \ll 1$ ),  $E_y \times B_z$  drift



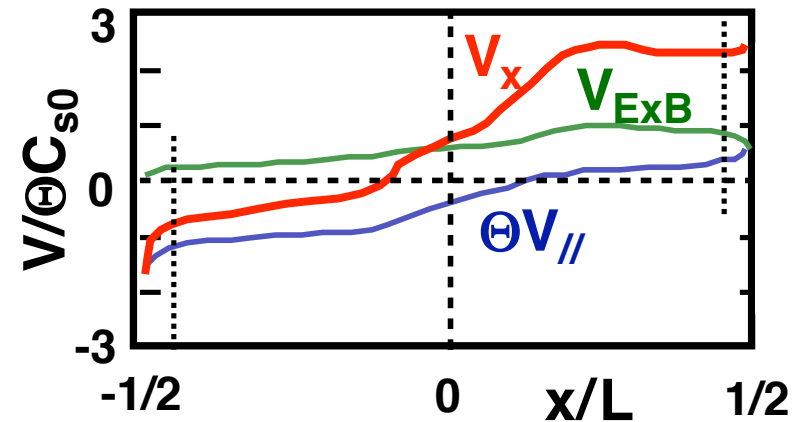
$$m_i V_x^2 \geq \Theta^2 T_{\text{eff} //}$$

$$V_x = \Theta V_{//} + V_{\text{ExB}}$$

$$T_{\text{eff} //} = T_{e //} + \gamma_a T_{i //}$$



### 2D PARASOL simulation



$$m_i V_{x0} V_x^* \geq \Theta^2 T_{\text{eff}}$$

$$V_{x0} = \Theta V_{//} + V_{\text{ExB}}$$

$$V_x^* = V_{x0} + n' T_{e //} / n B$$

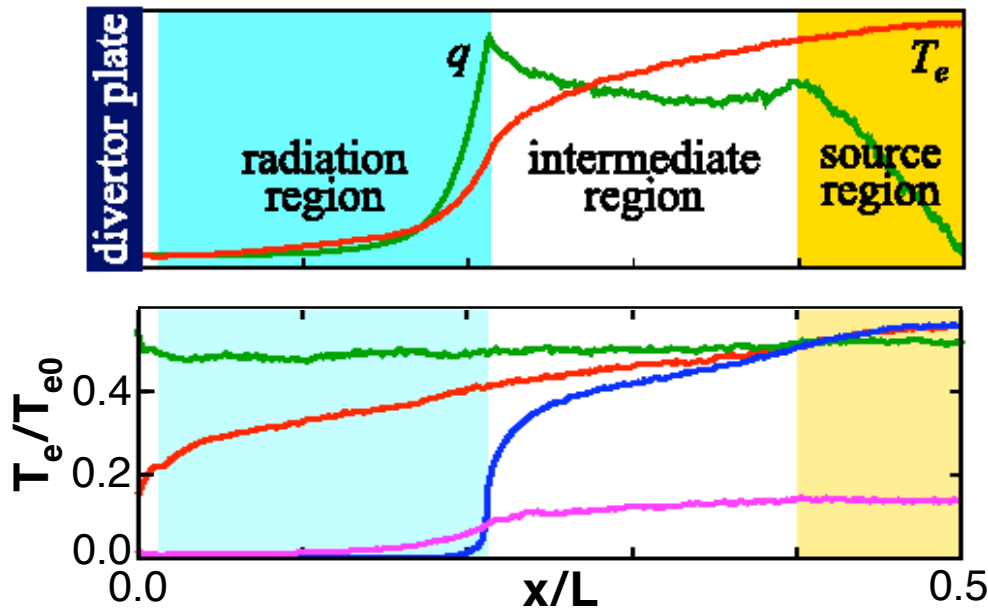
$$T_{\text{eff}} = T_{\text{eff} //} + (V_{//}' / \Theta \Omega) T_{\text{eff} \perp}$$

**1D** : T. Takizuka, M. Hosokawa, Contrib. Plasma Phys. **40** (2000) 471.

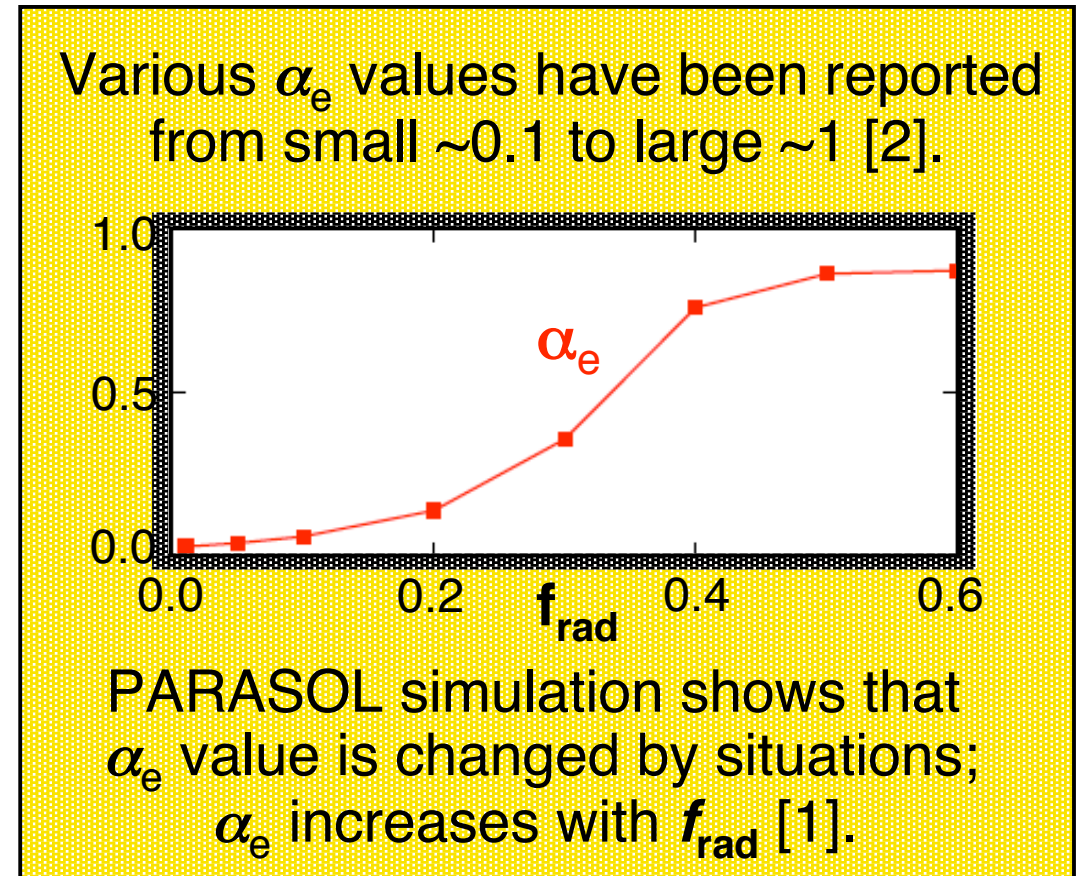
**2D** : T. Takizuka, M. Hosokawa, K. Shimizu, J. Nucl. Mater. **313-316** (2003) 1331.

# Kinetic effect on the parallel heat transport in SOL

**Collisional**  $l_{\text{mfp}} \ll L$     **Collisionless**  $l_{\text{mfp}} \gg L$     **Harmonic average model**  
 $q_{e//} = q_{\text{SH}} = -\kappa_{e//} dT_e/ds$      $q_{e//} = \alpha_e q_{\text{FS}} = \alpha_e n T_e v_{\text{eth}}$      $q_{\text{eff}}^{-1} = q_{\text{SH}}^{-1} + (\alpha_e q_{\text{FS}})^{-1}$



| $f_{\text{rad}}$ | $l_{\text{mfp}}/L$ |   | $f_{\text{rad}}$ | $l_{\text{mfp}}/L$ |   |
|------------------|--------------------|---|------------------|--------------------|---|
| 0.1              | $10^2$             | — | 0.5              | $10^3$             | — |
|                  | $10^{-2}$          | — |                  | $10^{-1}$          | — |

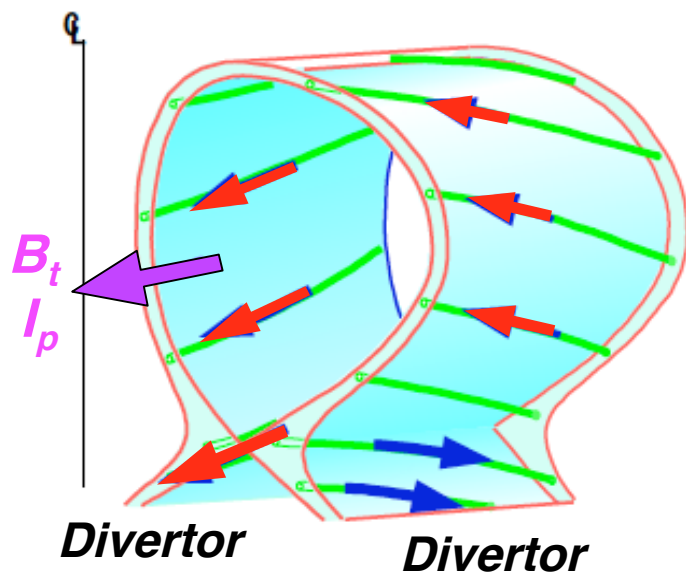
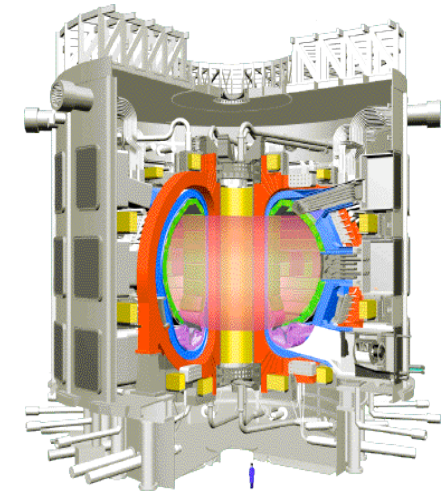


- [1] A. Froese, T. Takizuka, M. Yagi, "Electron parallel heat transport in the scrape-off layer using a particle-in-cell code", to be published in Plasma Fusion Res.
- [2] W. Fundamenski, Plasma Phys. Control. Fusion **47** (2005) R163.



# SOL Flow Pattern in Tokamaks

Plasma flow in the SOL plays an important role for the particle control in fusion reactors, such as ITER. The flow is expected to expel Helium ashes and to retain impurities in the divertor region, if it is directed towards the divertor plate.



It has been experimentally observed, however, that the flow direction is sometimes opposite; from the plate side to the SOL middle side in the outer SOL region (low field side) of tokamaks. This backward flow is seen when the single null point is located in the ion  $\nabla B$  drift direction.

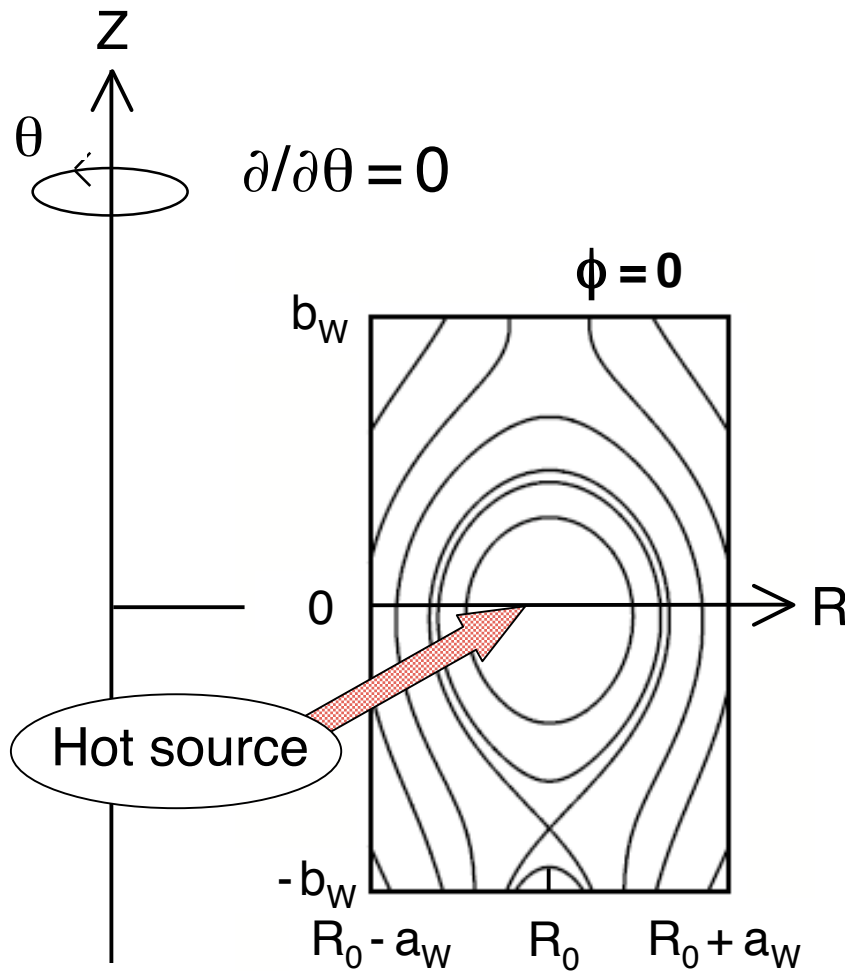
Physics mechanisms of this backward flow have not fully been known, though many simulation studies have been carried out with the fluid model.

Kinetic simulations are considered to bring a breakthrough on this subject. Kinetic models are able to simulate the effects of drifts, banana particles, self-consistent electric fields including sheath etc., which are considered to play important roles in the SOL flow formation.

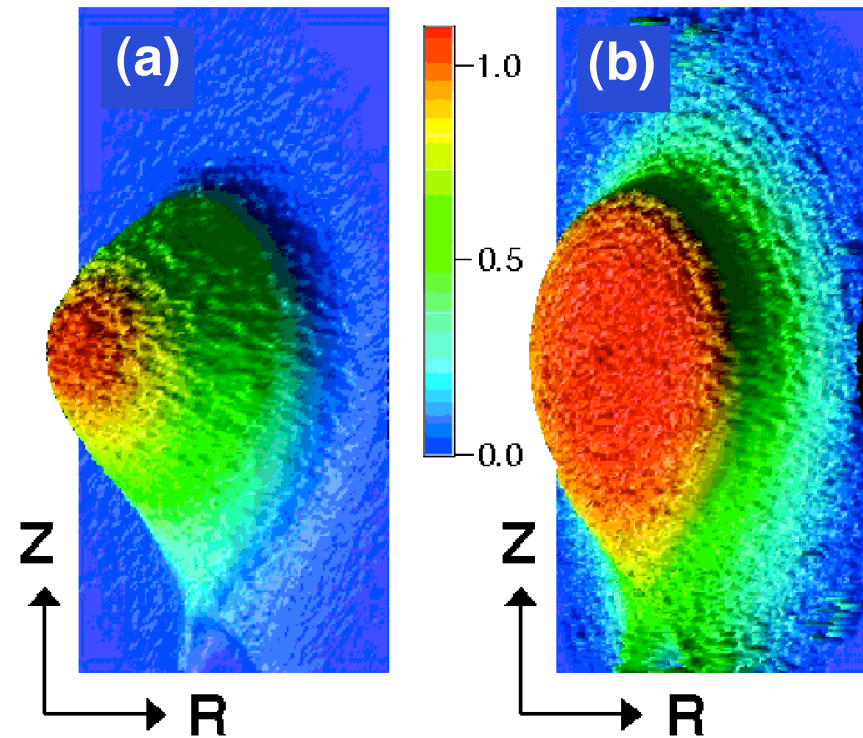
**Simulation study of the SOL flow patterns  
with a 2D full particle code PARASOL**

T. Takizuka et al., “Two-dimensional full particle simulation of the flow patterns in the scrape-off-layer plasma for upper- and lower- null point divertor configurations in tokamaks”, to be published in Nucl. Fusion

# 2D Toroidal PARASOL simulation

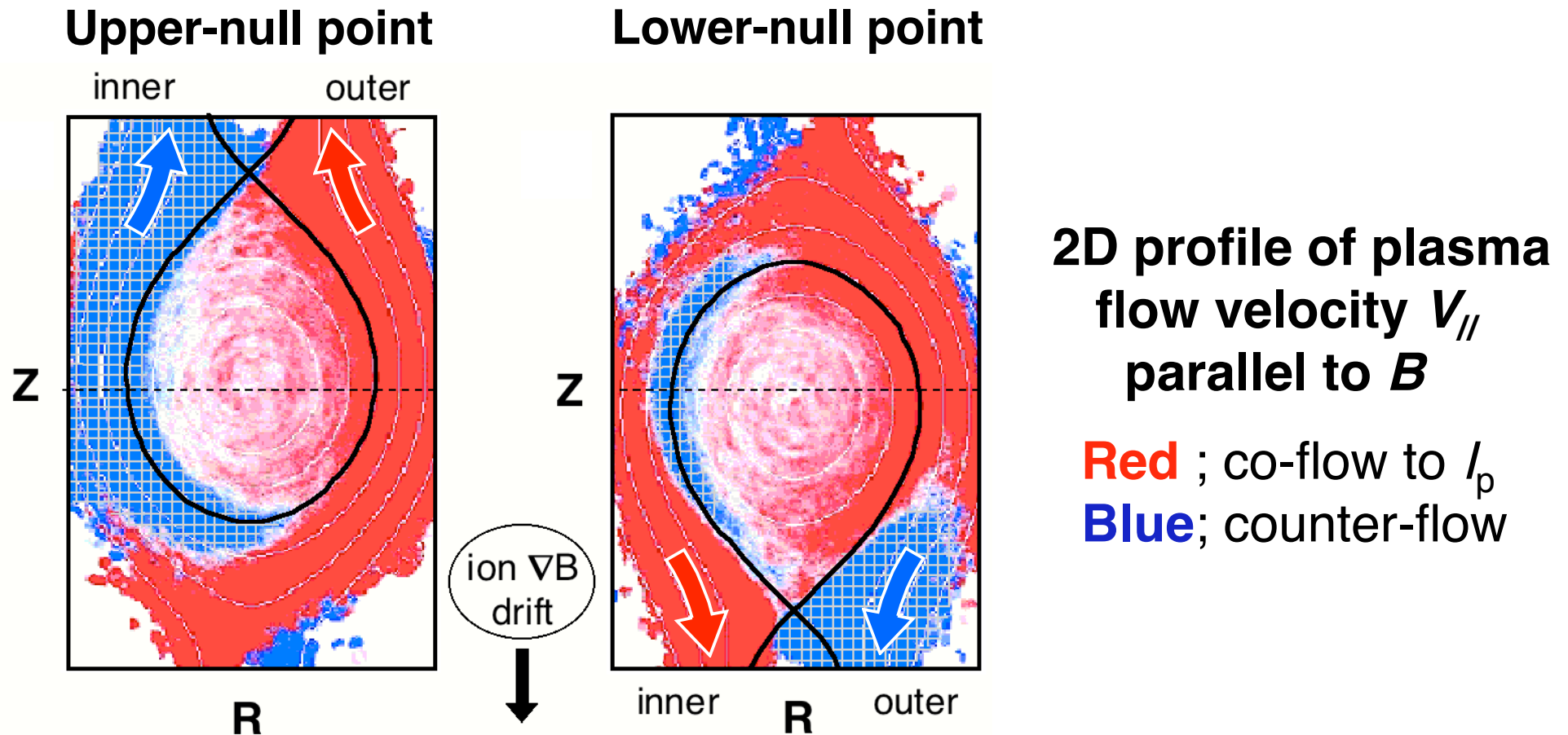


Stationary profiles of  
 $n_e$  and  $T_e$



$N_{i0} = 10^6$ ,  $M_R \times M_Z = 320 \times 512$ ,  $m_i/m_e = 400$ ,  $\rho_i/a \approx 0.02$ ,  $D \approx 10^{-5} a C_s$ ,  
 $l_{\text{mpf}}/L_{//} \approx 1$ ,  $\Theta = 0.2$  ( $q$  is not constant for the change of  $A = R_0/a$ )

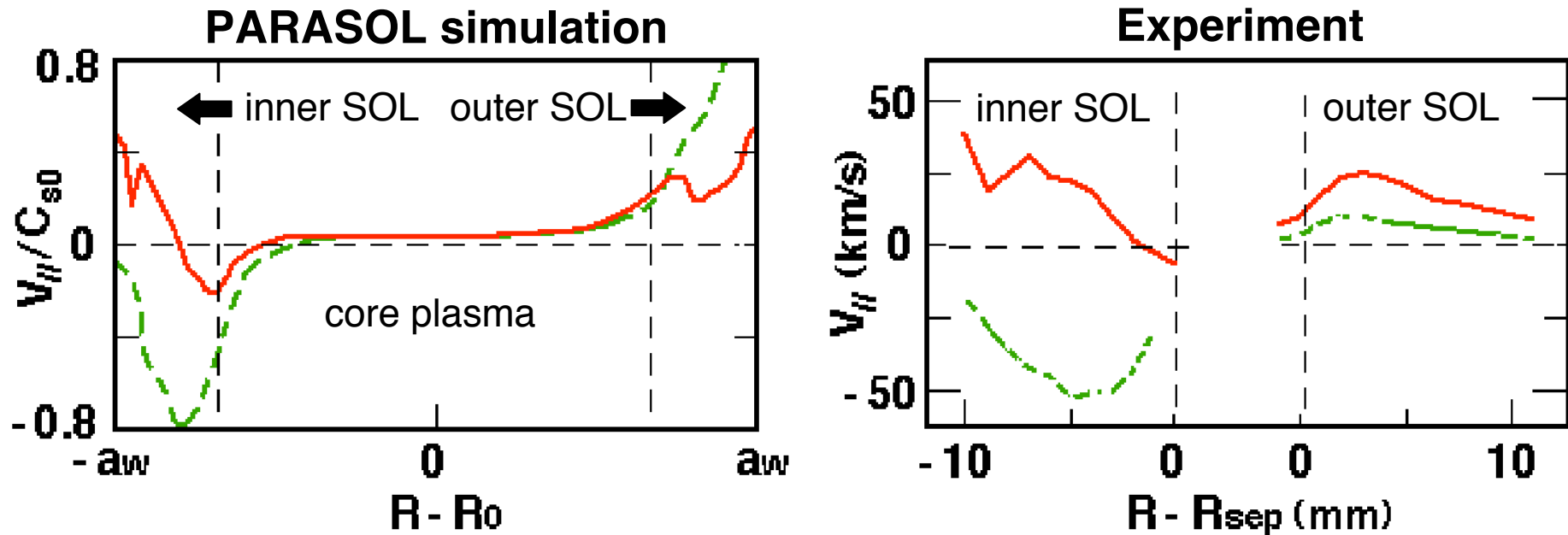
# SOL Flow Pattern for $A = 5.5$



**UN** : SOL flow  $V_{//}$  towards the both diverter plates.  
Stagnation point ( $V_{//} = 0$ ) symmetric at the bottom.

**LN** : Backward flow pattern in the outer SOL.  
Stagnation point below the mid-plane of the outer SOL.  
Island of the backward flow in the inner SOL.

# Comparison with Experiment : Similar Results



## Radial profiles of $V_{||}$ for UN and LN

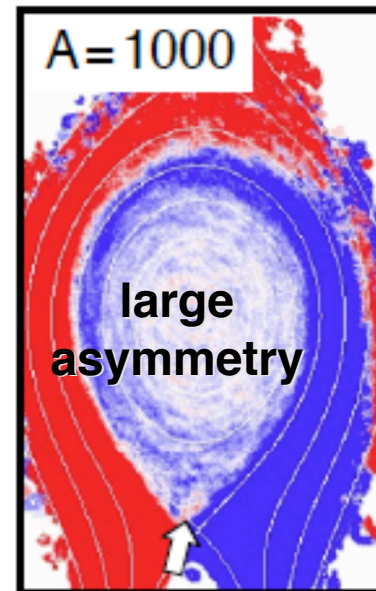
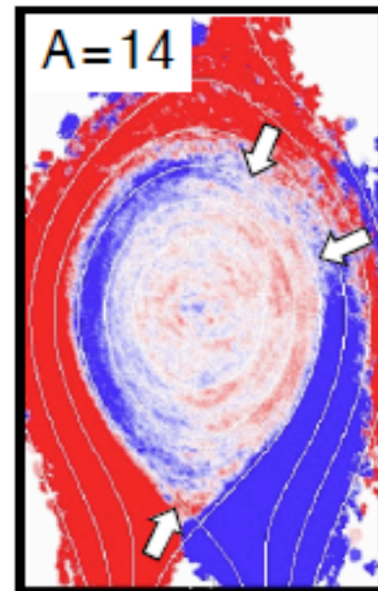
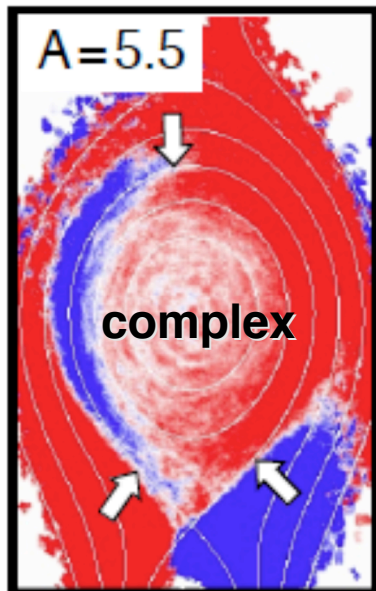
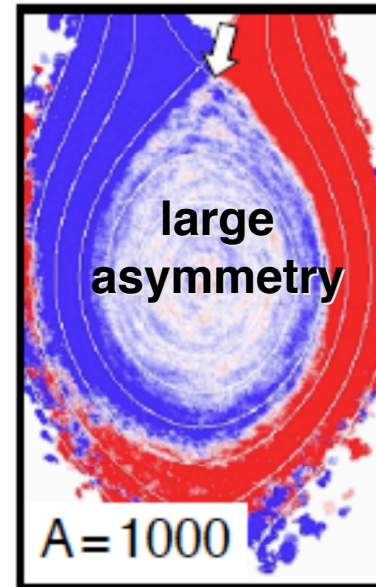
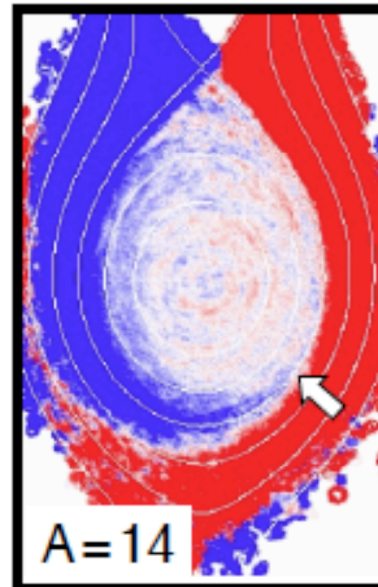
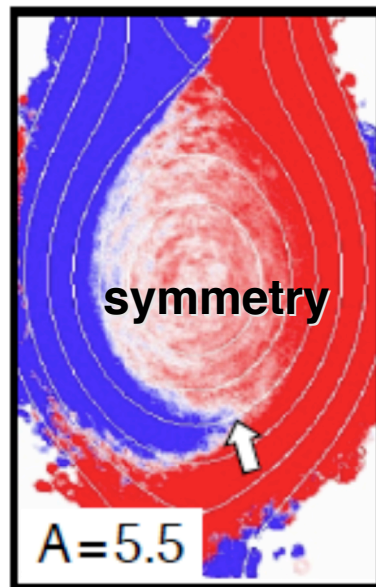
PARASOL simulation results (along the dotted line in former page) are very similar qualitatively and quantitatively to the experimental results of Alcator C-Mod


( B. LaBombard et al, Nucl. Fusion **44** (2004) 1047 )

$C_s \approx 50$  km/s ( $T = 30$  eV) and  $\rho_B \approx 5$  mm ( $T_i = 100$  eV,  $B_t = 5$  T,  $q = 4$ ,  $A = 3$ )

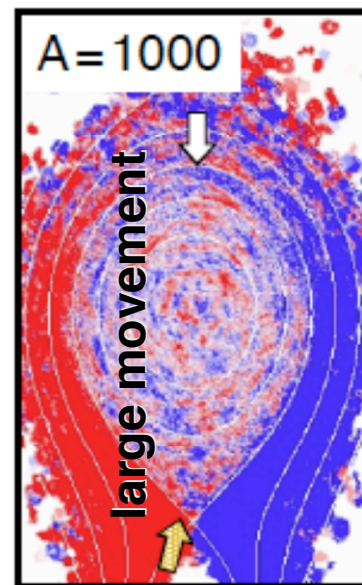
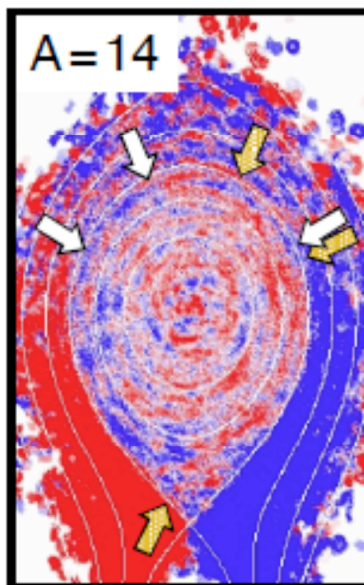
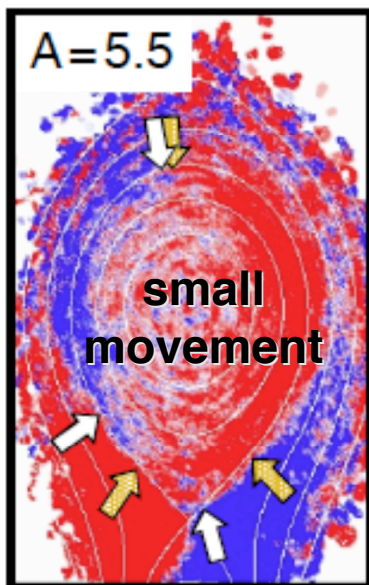
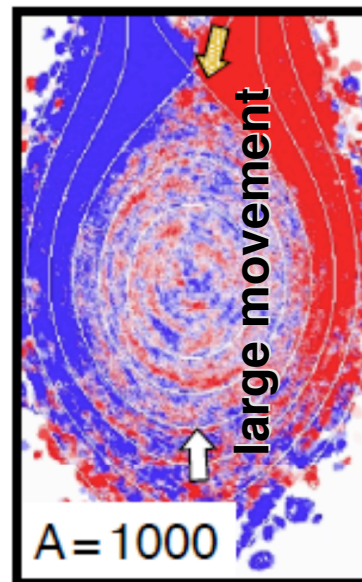
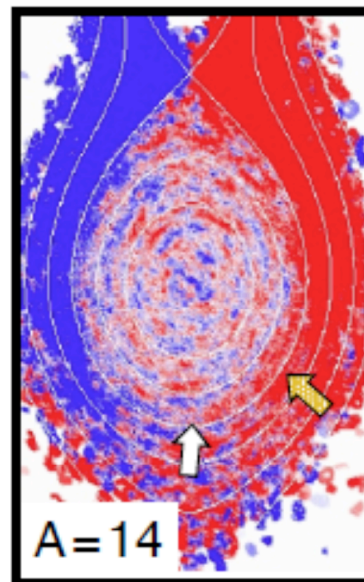
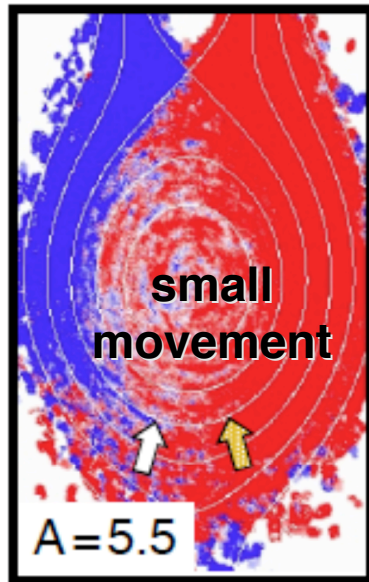


# Aspect Ratio Dependence ( $\Theta = \text{const.}$ )



Flow pattern  
and  
Stagnation point 

# Artificial Simulations without Electric Field



Flow pattern  
and  
Stagnation point

↑ Full simulation

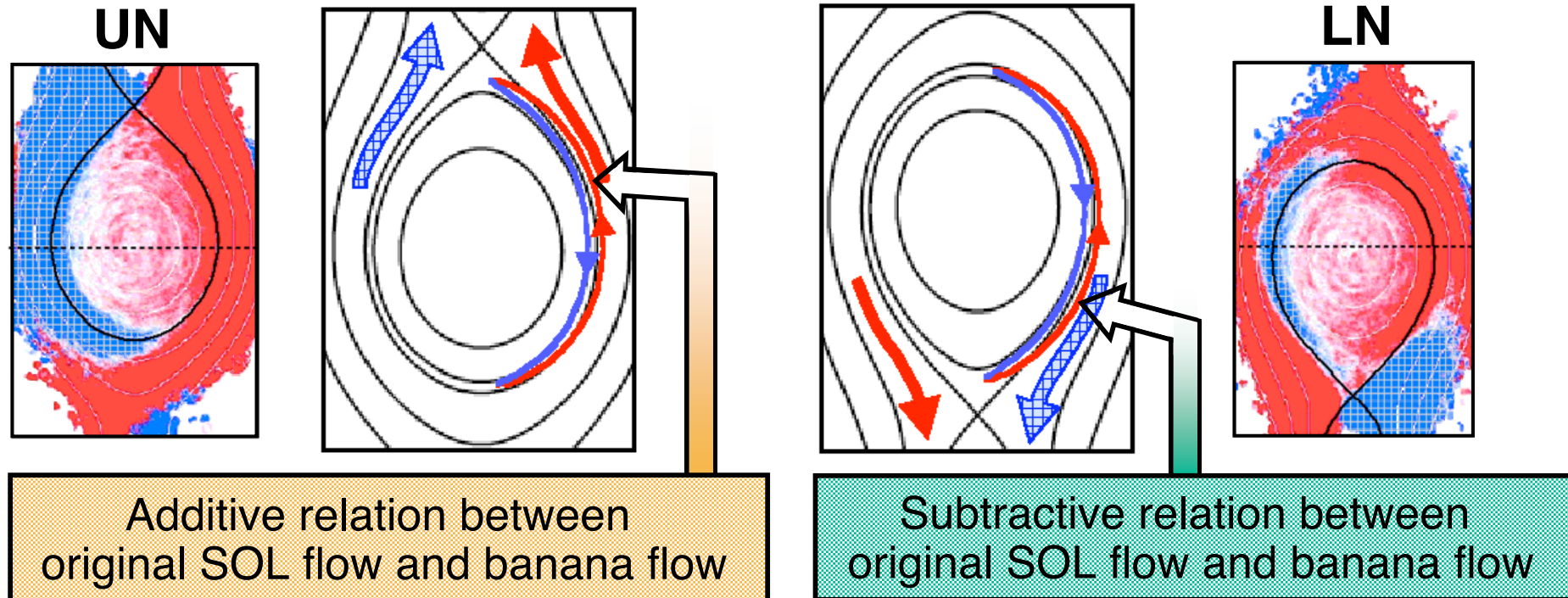
↑  $E=0$  simulation

When  $E=0$ ,  
plasma flow is  
determined only  
by ion motions.



Banana motion of trapped ions is essential for the formation of flow pattern in addition to the self-consistent electric field.

The effect of trapped ions can be stronger than the effect of electric fields for the standard tokamaks with  $A < 5$ .



**Based on these PARASOL results, it is required to develop a model of the trapped-ion induced flow in the edge plasma for comprehensive divertor simulations with the fluid model.**

T. Takizuka et al., "Modelling of ion kinetic effects for SOL flow formation", to be presented at 12th PET, Rostov, Russia, 2-4 Sep. 2009.



# Thanks to audiences and organizers



## Thanks to collaborators

K. Shimizu, M. Hosokawa, H. Kawashima, K. Hoshino, N. Hayashi,  
M. Honda, T. Ozeki, M. Yagi, A. Froese, K. Ohya, A. Fukuyama